



**HAL**  
open science

## Surface Treatment of Biochar-Methods, Surface Analysis and Potential Applications: A Comprehensive Review

Marlena Geça, Ahmed Khalil, Mengqi Tang, Arvind Bhakta, Youssef Snoussi, Piotr Nowicki, Malgorzata Wiśniewska, Mohamed Chehimi

### ► To cite this version:

Marlena Geça, Ahmed Khalil, Mengqi Tang, Arvind Bhakta, Youssef Snoussi, et al.. Surface Treatment of Biochar-Methods, Surface Analysis and Potential Applications: A Comprehensive Review. *Surfaces*, 2023, 6 (2), pp.179-213. 10.3390/surfaces6020013 . hal-04310222

**HAL Id: hal-04310222**

**<https://hal.science/hal-04310222v1>**

Submitted on 27 Nov 2023

**HAL** is a multi-disciplinary open access archive for the deposit and dissemination of scientific research documents, whether they are published or not. The documents may come from teaching and research institutions in France or abroad, or from public or private research centers.

L'archive ouverte pluridisciplinaire **HAL**, est destinée au dépôt et à la diffusion de documents scientifiques de niveau recherche, publiés ou non, émanant des établissements d'enseignement et de recherche français ou étrangers, des laboratoires publics ou privés.

Type of the Paper (Article.)

# Surface treatment of biochar: methods, surface analysis and potential applications. A comprehensive review

Marlena Geça<sup>1</sup>, Ahmed M. Khalil<sup>2,3,\*</sup>, Mengqi Tang<sup>3</sup>, Arvind K. Bhakta<sup>3</sup>,  
Youssef Snoussi<sup>3</sup>, Piotr Nowicki<sup>4</sup>, Małgorzata Wiśniewska<sup>1\*</sup>,  
Mohamed M. Chehimi<sup>3,\*</sup>

<sup>1</sup> Department of Radiochemistry and Environmental Chemistry, Institute of Chemical Sciences, Faculty of Chemistry, Maria Curie-Skłodowska University in Lublin, M. Curie-Skłodowska Sq. 3, 20-031 Lublin, Poland;

<sup>2</sup> Photochemistry Department, National Research Centre, Dokki, 12622 Giza, Egypt

<sup>3</sup> Université de Paris, CNRS, ITODYS (UMR 7086), 75013 Paris, France

<sup>4</sup> Department of Applied Chemistry, Faculty of Chemistry, Adam Mickiewicz University in Poznań, Uniwersytetu Poznańskiego 8, 61-614 Poznań, Poland

## Abstract:

In recent years, biochar has emerged as a remarkable biosourced material for addressing global environmental, agricultural, biomedical, and energy challenges. However, the performances of biochar rest in part on finely tuning its surface chemical properties, intended to obtain specific functionalities. In this review, we tackle the surface treatment of biochar with silane and other coupling agents such as diazonium salts, titanates, ionic/non-ionic surfactants, as well as nitrogen-containing (macro)molecules. We summarize the recent progress achieved mostly in the last five years and correlate the nature and extent of functionalization to eye catchy end applications of the surface-engineered biochar.

**Keywords:** Biomass conversion; Thermochemical treatment; Surface chemical modification; Coupling agents; Biochar implementation.

## Corresponding authors:

Mohamed M. Chehimi (UPC, [mohamed.chehimi@cnrs.fr](mailto:mohamed.chehimi@cnrs.fr)),

Małgorzata Wiśniewska (UL, [malgorzata.wisniewska@mail.umcs.pl](mailto:malgorzata.wisniewska@mail.umcs.pl)),

Ahmed M. Khalil (NRC, [akhalil75@yahoo.com](mailto:akhalil75@yahoo.com)).

# Graphical abstract

## Surface treatment of biochar: methods, surface analysis and potential applications. A comprehensive review

Marlena Gęca<sup>1</sup>, Mengqi Tang<sup>2</sup>, Ahmed M. Khalil<sup>2,3,\*</sup>, Arvind K. Bhakta<sup>2</sup>,  
Youssef Snoussi<sup>2</sup>, Piotr Nowicki<sup>4</sup>, Małgorzata Wiśniewska<sup>1\*</sup>,  
Mohamed M. Chehimi<sup>2\*</sup>

<sup>1</sup> Department of Radiochemistry and Environmental Chemistry, Institute of Chemical Sciences, Faculty of Chemistry, Maria Curie-Skłodowska University in Lublin, M. Curie-Skłodowska Sq. 3, 20-031 Lublin, Poland;

<sup>2</sup> Université de Paris, CNRS, ITODYS (UMR 7086), 75013 Paris, France

<sup>3</sup> Photochemistry Department, National Research Centre, Dokki, 12622 Giza, Egypt

<sup>4</sup> Department of Applied Chemistry, Faculty of Chemistry, Adam Mickiewicz University in Poznań, Uniwersytetu Poznańskiego 8, 61-614 Poznań, Poland



## 1. Introduction and scope of the review

It is without any doubt that biochar is a very hot topic, due to its central position, at the crossroads of materials science, materials and surface chemistry, surface science, catalysis, and organic reactions. Biochar is at the heart of sustainable development, and concerns biomass and waste valorization, and utilization for depollution and soil amendment. Such an infatuation for biochar is motivated by the availability of numerous varieties of biomasses and wastes worldwide, and the need for valorization and/or transformation into functional materials. This resulted in skyrocketing number of publications, exceeding 5500 since 2021.

The most important applications of biochar concern soil amendment and agriculture<sup>1-3</sup>, but recently much has been achieved in the design of biochar-supported nanocatalysts for water treatment consisting of total mineralization of organic pollutants such as dyes and drugs<sup>4, 5</sup>, or for reductive process,<sup>6</sup> or for catalyzing organic chemistry reactions.<sup>7, 8</sup> Other applications concern the use of biochar as fillers in composite materials<sup>9-11</sup>, electrode materials<sup>12, 13</sup> and for the developments of novel engineered biochar for the treatment of neglected tropical diseases (NTDs)<sup>14, 15</sup>, to name but these applications.

Whilst biochar can be employed as freshly obtained by thermochemical conversion of the biomass, it nevertheless requires particular surface treatment in order to impart it with new functionalities. In this mini-review, the focus is on the functionalization of biochar with molecular/macromolecular surface modifiers or coupling agents and catalytic nanoparticles, regardless of any pretreatment of the biomass or post-treatment of the biochar, or conducting pyrolysis under various gases such as N<sub>2</sub>, N<sub>2</sub>/H<sub>2</sub>,<sup>16</sup> or CO<sub>2</sub>,<sup>8</sup> NH<sub>3</sub>, etc. For more details about specific activation strategies of biochar, the reader is referred to the shortlisted reviews gathered in Table 1.

**Table 1. Shotlisted, relevant reviews tackling applications of surface engineered biochar**

Running title	Review main topic	Year review published	References
Biochar for catalytic biorefinery and environmental processes	The article summarizes the knowledge on the production of biochar, its classical activation with aggressive compounds and its use to expediate biorefinery operations and degradation of environmental pollutants	2019	17
Chemically modified carbonaceous adsorbents for CO <sub>2</sub> capture	The review discusses activation, surface amination or carboxylation, and doping of various carbon allotropes, including biochar, for extensive capture of CO <sub>2</sub> .	2021	18
Biochar as a support for nanocatalysts and other reagents	The review paper summarizes the knowledge on the use of biochar-supported nanocatalyst, and discusses the mode of coordination of the catalyst nanoparticles by the biochar.	2021	19
Phosphorus adsorption by functionalized biochar	Inefficient crop fertilization induces water pollution by phosphorus. The review discusses biomass pre-treatment as well as post-modification of biochar to obtain efficient phosphorus porous adsorbents	2022	20
Surface modification of biochar for dye removal	The review discusses several strategies of obtaining functional biochar for the removal of dyes from water.	2022	21
Biochar for the removal of contaminants from industrial wastewaters	The paper reviews methods for obtaining pristine and engineered biochar for the efficient removal of numerous contaminants from industrial wastewaters.	2022	22
Biochar as a reinforcing bio-based filler in rubber composites.	This article is focussed on the key properties of highly reinforcing fillers such as particle size, structure, and surface activity. The review essentially covers silane modification of biochar.	2023	10

These reviews concerned various carbon allotrope surface modification<sup>18</sup>, classical activation methods<sup>17</sup> that rest on acid or alkali treatment of biochar, activation with metal chlorides, and post pyrolysis under steam to name but a few. However, despite the numerous advances in biochar production, post-modification, and applications, only a few reviews covered surface modification, for example, the surface treatment of biochar particles with silanes for the design of high performance composites (see Table 1). Coverage of the chemical modification of biochar surface with a large series of well-known coupling agents such as silanes, diazonium salts, aminated compounds, surfactants and macromolecules is lacking despite its interest in several domains, *i.e.* organic chemistry, polymer science and technology, environmental remediation, and sustainable energy. This is what has motivated this review article.

## 2. Biomass conversion to biochar

Biochar and other related porous carbon materials can be obtained by conversion of biomass using pyrolysis, under an inert or reducing atmosphere. Figure 1 displays the impact of pyrolysis parameters on the types of products obtained.<sup>23-26</sup> Slow pyrolysis is the recommended technique for obtaining biochar.

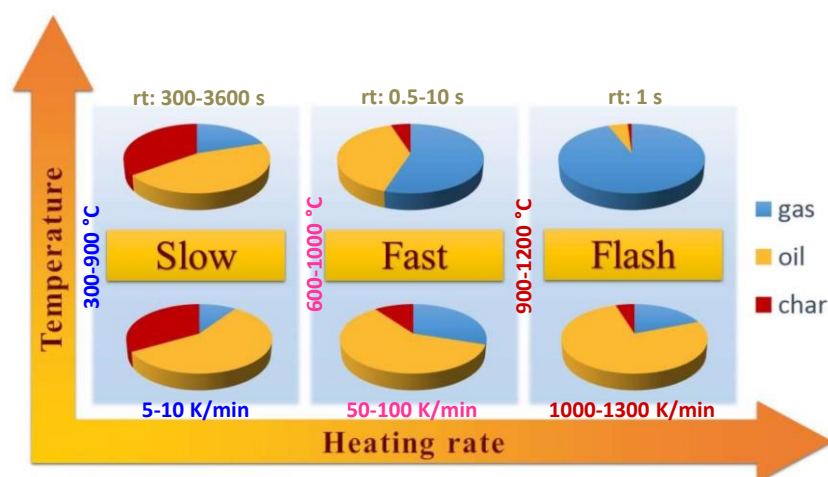


**Figure 1.** Pyrolysis techniques and the effect of process parameters on product distribution (*rt*: residence time). Adapted from<sup>26</sup>.

Carbonization could also be achieved through different processes namely hydrothermal treatment to produce hydrochar,<sup>27</sup> microwave-assisted carbonization,<sup>28</sup> laser-induced biochar elaboration,<sup>29</sup> gasification,<sup>30</sup> and torrefaction.<sup>31</sup>

The biochar-making method governs its textural and structural properties, and chemical composition. These characteristics decide the potential application of the carbonaceous matter. For example, microwave pyrolysis is recommended for applications like adsorption and heterogeneous catalysis; indeed, the latter require pronounced porous structure and high specific surface area. Moreover, increased yield of high quality biochar could be obtained by microwave pyrolysis, compared to the conventional pathways.<sup>32</sup> Gasification based on a partial

oxidation of the bio-feedstock using carbon dioxide, oxygen, air, steam or a mixture of these gases, promotes the production of syngas/producer gas, resulting in a relatively low biochar yield in the 5-10 percentage range.<sup>33</sup> The pyrolysis conditions (temperature, residence time) of biomass are known to be the key factor controlling the polycyclic aromatic hydrocarbons (PAHs) and volatile organic compounds (VOCs) content in biochar, then, their control is crucial to monitor the release of PAHs and VOCs from the carbonized biomass in soil amendment application.<sup>34, 35</sup>

Besides the conversion method, the initial biomass could be mixed with ZnCl<sub>2</sub> or KOH, or H<sub>3</sub>PO<sub>4</sub> (used before or after pyrolysis) in order to control the biochar yield and textural properties.<sup>23</sup> As noted above, the gas used during pyrolysis has a major effect on the chemical structure. For example, the mixture N<sub>2</sub>/H<sub>2</sub> induces less oxygen in the final biochar, and a higher isoelectric point (IEP) compared to the same biochar obtained using pure N<sub>2</sub>.<sup>16</sup> Textural properties could be controlled via green approaches consisting in mechanical grinding<sup>36</sup> or maceration of the initial biomass in water/alcohol mixture.<sup>15</sup> We have recently noted that the preparation of biochar@nickel composite by pyrolysis of biomass impregnated with nickel salt induced an unusual fishnet-like structure of biochar.<sup>37</sup> Actually, nickel catalyzes the carbonization of the biomass and leads to a more porous biochar structure.<sup>38</sup>

### 3. Biochar surface treatment pathways

#### 3.1. General aspects

Figure 2 schematically illustrates shortlisted pathways for chemical modification of biochar surface. The literature survey using Google Scholar and the Web of Science indicated that the most employed compounds are silane coupling agents, ionic or non-ionic surfactants, and aryl diazonium salts. For catalytic purposes, titanates have also been proposed. Silanes require hydroxylated surfaces and thus are applicable to biochar as most biochar materials are prepared by thermochemical conversion at 300-500 °C, a range of temperature that ensures the presence of reactive functional groups such as OH and C=O.<sup>21</sup> Such groups can also be obtained by post acidic treatment.<sup>21, 39</sup> Concerning diazonium salts, most carbon allotropes react with these modern surface modifiers to provide C-C bonds and ester linkages.<sup>40</sup> As far as surfactants are concerned, anionic and cationic surfactants interact with biochar via completely different mechanisms (biochar-hydrophobic tail, or biochar-hydrophilic head)<sup>41</sup>. Non-ionic surfactants have completely different behaviour and rather interact with biochar via oxygen atoms or OH groups (see Section 3.4). Titanates are able to form TiO<sub>2</sub> nanoparticles, in situ, at the surface of biochar and are thus important for providing photocatalytic composites.<sup>42</sup> Other emerging coupling agents are polyethyleneimine (PEI).<sup>43</sup>

In this review, we concentrate on coupling agents that react/interact chemically with biochar, via covalent linkages or through strong electrostatic interactions, hydrogen bonds, or hydrophobic interactions.

Other strategies consisting of direct immobilization of nanocatalysts on biochar obtained by pyrolysis of biomass impregnated with metal salt precursor will be briefly summarized at the end of the review.

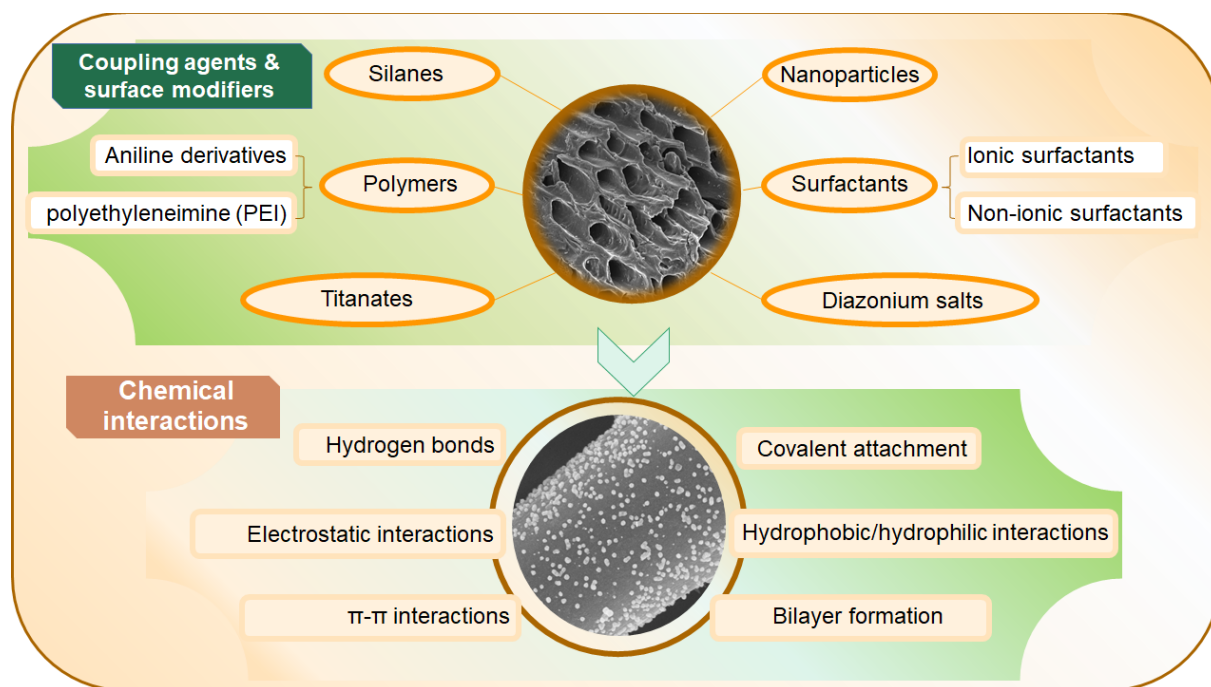


**Figure 2.** Schematic illustration of biochar surface treatment with popular coupling agents.

### 3.2. Surface functionalization with silane coupling agents

Silanization is the process of modification of surfaces by incorporating organofunctional alkoxy silane.<sup>44</sup> The reaction is usually conducted in aqueous or hydro-alcoholic media. The important steps in silanization are<sup>45</sup>: (i) silane hydrolysis which leads to  $R-Si(OH)_3$ , (ii) hydrogen bonding between the hydrolyzed silane and the surface, (iii) condensation with the surface resulting in surface-O-Si linkage, (iv) possible polymerization of the silane in solution, and (v) reaction with pending R group with other species as will be briefly discussed below.

In the case of biochar, the abundance of -OH functional groups is crucial for its functionalization with silane coupling agents. Such a modification permits the fabrication of high-performance biochar-filled polymer composites, immobilized catalysts, and metal complexes, materials for electromagnetic shielding and road engineering among numerous applications. We will select a few case studies of distinct types of applications in order to show the possibilities offered by silanes to impart new functionalities and performances to biochar.



Figure 3a depicts a general pathway of functionalization of biochar that bears surface hydroxyl groups. The group R borne by the silane is chosen in a way it imparts a specific functionality to biochar: post-functionalization, hydrophilic/hydrophobic interactions, metal complexation/chelation, in situ polymerization, and dispersion in polymer matrix. Indeed, modified biochar can be used to make composite membranes for pervaporation, a process that uses a poly(dimethyl siloxane) (PDMS) for the separation of ethanol/water mixture.<sup>46</sup> Figure 3b shows the steps involved in biochar silanization. Firstly, silanes go through hydrolysis, followed by condensation to produce oligomers. Finally, oligomers react with -OH groups on biochar surface, thus leading to biochar-O-Si covalent bonds.<sup>47</sup> Pending methoxy groups react with PDMS which results in biochar/PDMS composite membrane. Vinyl-silanized biochar imparts superior hydrophobic properties to the PDMA membrane compared to aminosilane, as the latter interact favourably with water due to its free amine group.<sup>46</sup>

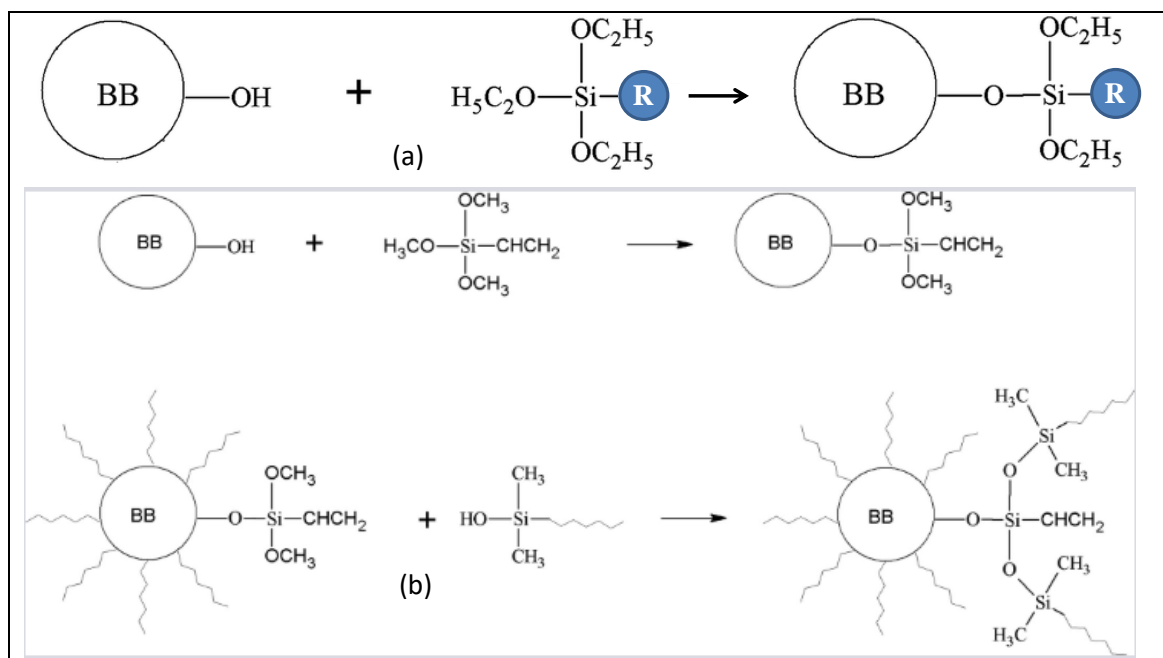


**Figure 3.** (a). General pathway for the silanization of biochar. R= -(CH<sub>2</sub>)<sub>3</sub>NH<sub>2</sub>, -(CH<sub>2</sub>)<sub>3</sub>Cl, -(CH<sub>2</sub>)<sub>3</sub>SH, -(CH<sub>2</sub>)<sub>3</sub>O-(C=O)-(C=CH<sub>2</sub>)CH<sub>3</sub>, -CH=CH<sub>2</sub>. ...

(b) Silanization of wood biochar with vinylsilane, followed by reaction with PDMS. Reproduced from<sup>46</sup> with permission of John Wiley & Sons.

Silanization of the surface with aminosilane (Figure 4), followed by condensation, led to a removal capacity of CO<sub>2</sub> 3.7 mmol/g (specific surface area SSA= 394 m<sup>2</sup>/g), higher than 3.4 mmol/g, obtained with Norit, a commercial product of which SSA=3.4 mmol/g.<sup>48</sup>

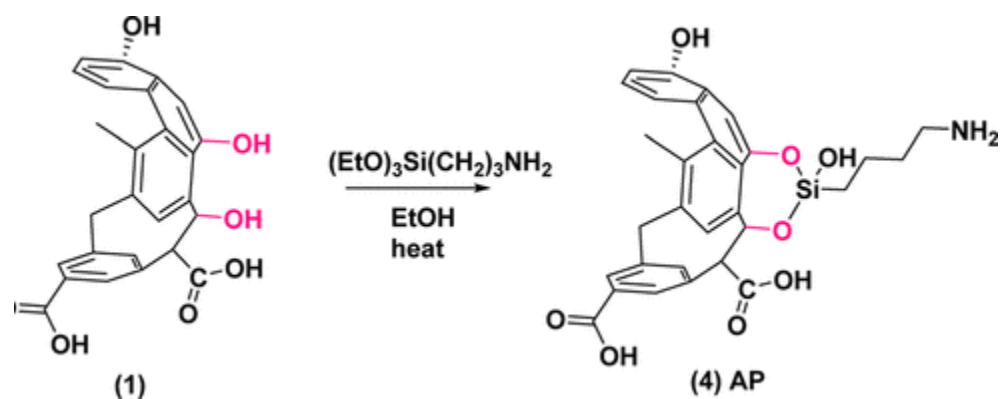


**Figure 4.** Modification of biochar surface with aminosilane coupling agent. Reproduced from <sup>48</sup> with permission of ACS.

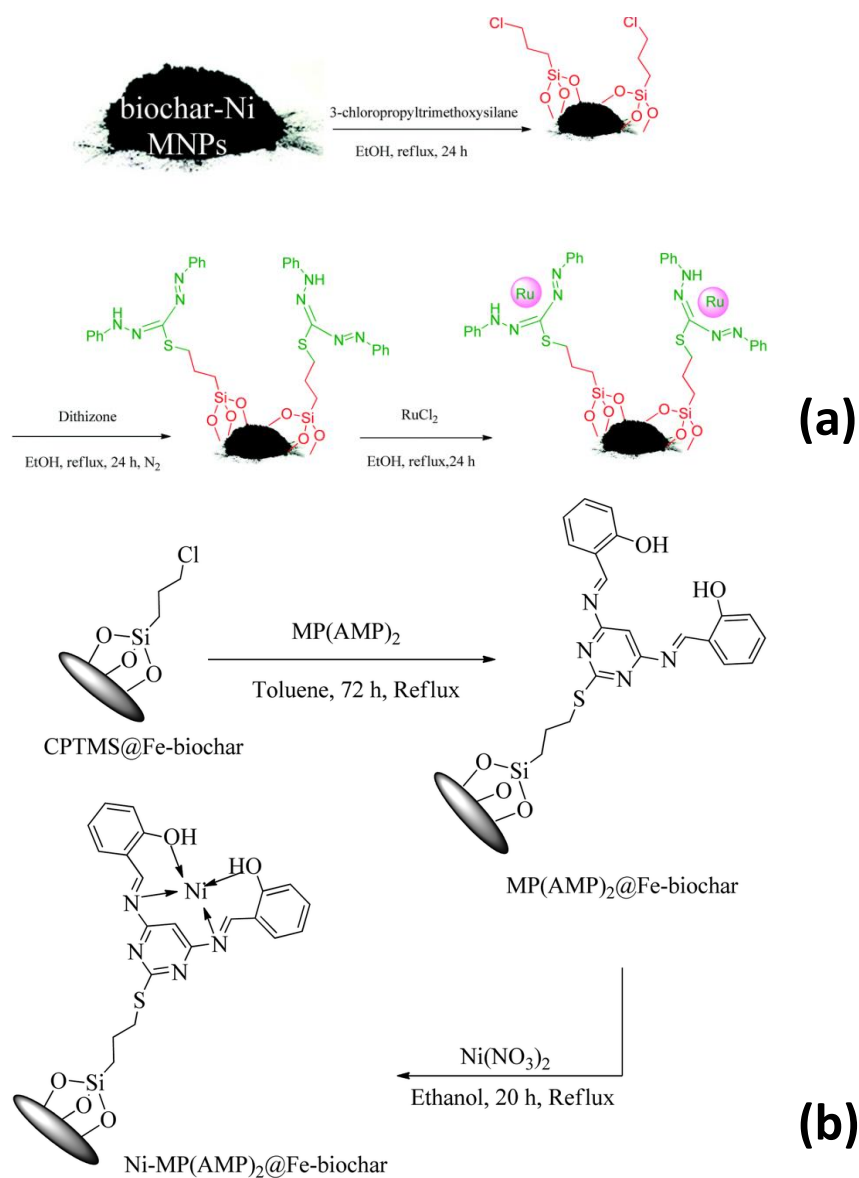
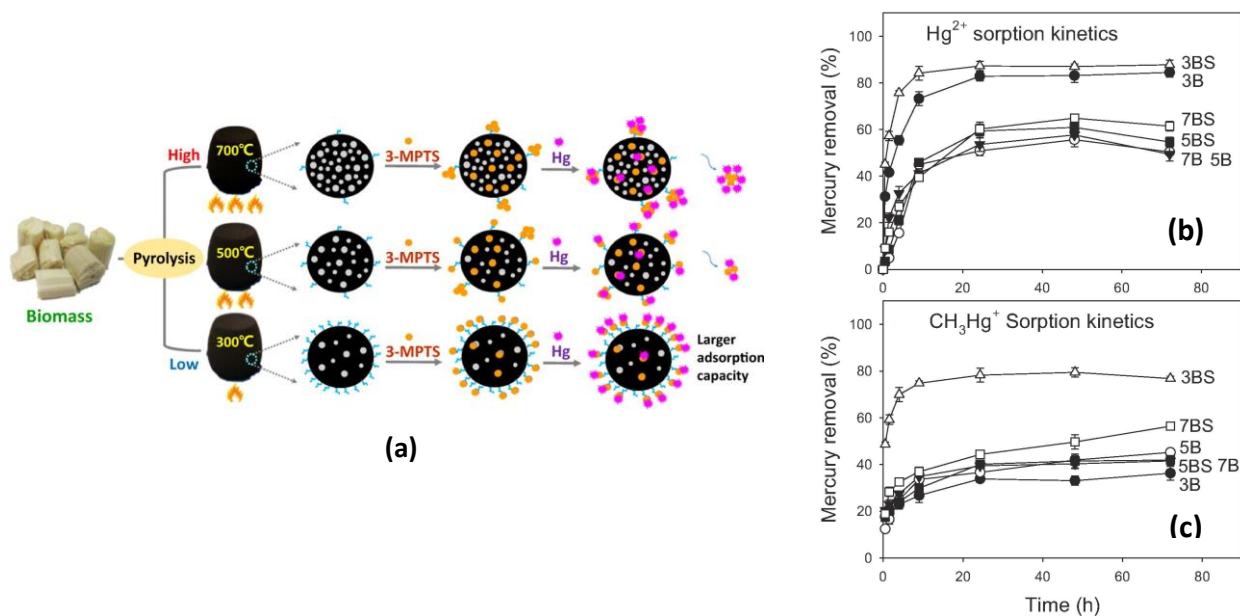


**Figure 5.** Strategies to design silanized biochar for the immobilization of heterogeneous catalysts of organic chemical reactions: Biochar@Ni modified with silane for covalent coupling of ruthenium ligand (a), and chloro-silanized biochar, post-modified with mercaptan derivative for

chelating nickel catalyst (b). (a) Reproduced with permission of RSC, from <sup>49</sup>(a), and from <sup>50</sup>(b).

Silanization could be an important step to enable the post-functionalization of biochar, with complex structures such as metal chelators. Figure 5 depicts a strategy for anchoring ruthenium (Figure 5a), iron, and nickel-containing moieties (Figure 5b). They have exhibited enhanced catalytic activity with high turnover frequency for organic reactions.

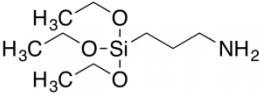
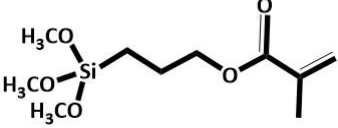
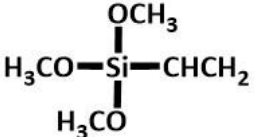
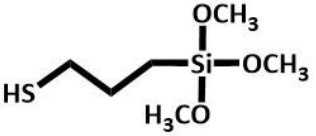
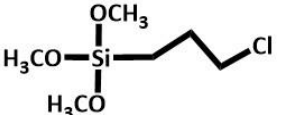
If silanization permits to impart new functionality to biochar, spatial distribution of the surface-bound reactive groups is an issue. For example, Huang *et al.*<sup>51</sup> have brought strong supporting evidence for the effect of pyrolysis temperature on the silanization extent of pine sawdust biochar; they have shown that mercapto-silanization was more efficient with the decreasing order of temperature 300 > 500 > 700 °C. Indeed, biochar has much more OH, C=O, and COOH groups at low pyrolysis temperature, therefore enabling even distribution of SH groups at the surface, resulting in larger removal of Hg(II) and  $\text{CH}_3\text{Hg}^+$  ions (Figure 6). Interestingly, the high-resolution S2p region from 3BS biochar (prepared at 300 °C and silanized) exhibited peak broadening due to the formation of mercury sulphide. Although 3B and 3BS samples exhibited the lowest specific surface area (1.7 and 4.2 m<sup>2</sup>/g, respectively), substantial mercury compounds could be removed (see Figure 6b,c). This is a clear indication that even and densely packed distribution of mercapto groups overcame the textural properties imparted by high pyrolysis temperature (335 and 235 m<sup>2</sup>/g for 7B and 7BS, respectively).



**Figure 6.** Fabrication of mercapto-silvanized biochar for the removal of Hg compounds. Schematic illustration of the pyrolysis temperature effect on silanization extent, textural and adsorption capacity of biochar (a); effect of pyrolysis temperature and silanization on the removal of Hg<sup>2+</sup> (b), and <sup>3</sup>HCHg<sup>+</sup> (c). Reproduced from<sup>51</sup> with permission of Elsevier.

Table 2 reports different silane coupling agents employed to modify biochar surfaces and their potential applications. It shows that either such silane-modified biochar or their further modification have been used for different purposes including water treatment, nanoparticles capture, polymer reinforcement, membranes, road engineering, land fill cover, etc.

**Table 2. Surface treatment of biochar with silanes coupling agents**

Coupling agent	Biomass	Surface treatment conditions	Properties of engineered biochar	Potential application	Refs.
 <p style="text-align: center;"><b>APTES</b></p>	Sawmill residues	Char/water=10/1; 2 wt.% APTES; condensation at pH 3-4 for 1h followed by reaction at 70 °C for 6h. Post-activation in air at 560 °C.	SSA=394 m <sup>2</sup> /g; 0.24 wt.% N;	CO <sub>2</sub> adsorption capacity of 3.7 mmol/g	48
	Oil sludge	C <sub>2</sub> H <sub>5</sub> OH: H <sub>2</sub> O: KH-550 ratio of 70: 25: 5, left for 60 min. Then, oil sludge pyrolysis residue added and stirred for 1 h, followed by drying at 60 °C. (KH-550: aminosilane)	Rheological properties (rutting resistance factor, creep stiffness, and high temperature performance) improvement of the asphalt mortar	Road engineering	52
	Onion peels	Silane (3 wt.%) was mixed with C <sub>2</sub> H <sub>5</sub> OH- H <sub>2</sub> O solution (95 wt % C <sub>2</sub> H <sub>5</sub> OH + water + acid 5%), stirred for 10 at room temp. Then, ball milled Co-biochar was incorporated, rinsed for 10 min and filtered, and finally dried at 110°C.	High tensile strength and  EMI: -44.37 dB and -49.62 dB for X and Ku band	PVA composite For EMI application	53
<b>KH-570</b> 	Rice straw	Mixture of pre-treated biochar + 20% (v/v) KH-570, 72% (v/v) absolute C <sub>2</sub> H <sub>5</sub> OH + 8% (v/v) H <sub>2</sub> O, magnetically stirred at 30°C, mixed with modifier for 12h, washed with ethanol, filtered and dried at 50°C.	Enhanced CH <sub>4</sub> oxidation	Soil cover for landfill gas control.	54
	Rice straw	-	H <sub>2</sub> O absorption =1.27 g (g biochar) <sup>-1</sup>  Water proofing, MOB growth promotion, ventilation and efficient CH <sub>4</sub> reduction.	Land fill cover soil	55
<b>YDH-171</b> 	lodgepole pine bark	Synthesized biochar at 600°C and modified by YDH-171. Further, 3 wt.% modified were taken for further experiment	PV performance: separation factor (11.3) and  flux (227.25 g m <sup>-2</sup> h <sup>-1</sup> ).	PV membranes (Separating C <sub>2</sub> H <sub>5</sub> OH from H <sub>2</sub> O.	46
<b>A-189</b> 	Bamboo	Pre-treated ultrafine bamboo char was mixed with A-189 (16 w/w%). Following silane treatment, oven-dried for 24 at 105 °C.	Tensile strength (18.87 MPa) and tensile modulus (272 MPa) increased by 99.3 % and 104.9%).	Polymer reinforcement	56
<b>CPTMS</b> 	Chicken manure	Pyrolyzed biomass (400-800 °C, 1 to 2h) was treated with CPTMS followed by dispersion in 1.5 mmol TBA and toluene and stirred for 48 h at 90°C. Residue was isolated, washed with C <sub>2</sub> H <sub>5</sub> OH and dried (50°C). Then, Pd (OAc) and NaBH <sub>4</sub> treatment at optimum condition.	In the synthesis of biphenyl derivatives (yield = 97%, TON = 135, and TOF = 405)	C-C coupling reaction (Suzuki-Miyaura and Heck-Mizoroki cross-coupling reactions.)	57

Biochar-Ni magnetic composite were refluxed with 1.5 silane in the presence of ETOH for 24 h. Several other steps followed by treatment with dithizone and RuCl <sub>2</sub> leads to formation of Ru-dithizone@biochar-Ni MNPs	High catalytic activity for C-C coupling reaction of iodobenzene or chlorobenzene with 96 % yield.	Suzuki C-C coupling reaction 49
CPTMS@Fe-biochar treated with MP(AMP) <sub>2</sub> and refluxed for 72 h in the presence of toluene and then the product is refluxed with ethanol and nickel nitrate for 20h.	Enhanced catalytic efficiency. Catalyst recovery through magnet. Homoselectivity was observed. %yield = 98%. Recyclable upto 9 times.	Catalysis ( synthesis of tetrazole derivatives) 50

---

APTES: aminopropyl triethoxysilane; EMI: electromagnetic interference shielding; PV: Pervaporation ; PVA: Poly vinyl alcohol; SSA: specific surface area; TOF: turnover frequency



### 3.3. Titanate surface modifiers

Titanates are well-known coupling agents in composite science and technology<sup>58, 59</sup> generally speaking, and more specifically in the domain of dental materials.<sup>60, 61</sup> They are proposed for the fabrication of robust dental composite materials.

They have been explored in surface modification of rice bran biochar, but without mention of potentially occurring surface reaction.<sup>42</sup> For this purpose, magnetic biochar was prepared by post-modification with Fe(II) and Fe(III) iron chlorides via pyrolysis, followed by sol-gel process synthesis of TiO<sub>2</sub> from titanate, in the presence of the magnetic biochar@Fe. The final material was applied for the photocatalyzed removal of tetracycline antibiotic and for antibacterial application. Of particular interest to surface and interface phenomena, Ti-O-C interfacial functional group was probed by FTIR, which accounts for the covalent attachment of TiO<sub>2</sub> to the underlying biochar.

In another study, titanates were used in order to modify preformed biochar in a sol-gel process. The titanate-modified biochar was pyrolyzed in order to obtain biochar@TiO<sub>2</sub>. Further wetting impregnation with silver nitrate followed by pyrolysis resulted in biochar@TiO<sub>2</sub>-Ag with antibacterial activity against *E. coli* (99% of sterilization ratio in 5 min, under daylight).<sup>62</sup>

XPS analysis was used to probe titanate interaction with carbon allotropes, but only rare examples have been found. For example, activated carbon was treated with titanate in order to design supercapacitors (specific capacitance: 376.2 F.g<sup>-1</sup>, internal resistance: 0.91 Ω).<sup>63</sup>

Although, not strictly on biochar, but of relevance to this review and the scope of the journal Surfaces, recently titanates were proposed for the covalent attachment of graphene oxide (Figure 7) in order to provide surface-bound alkyl groups that ensure dispersion of GO in hydraulic oils.<sup>64</sup> Interestingly, C1s spectra show a drastic decrease in the C-O component due to the covalent attachment of the long alkyl chains to the GO via titanium. Such surface-bound groups permitted excellent dispersion of titanate-modified GO in hydraulic oil with remarkably improved tribological properties.

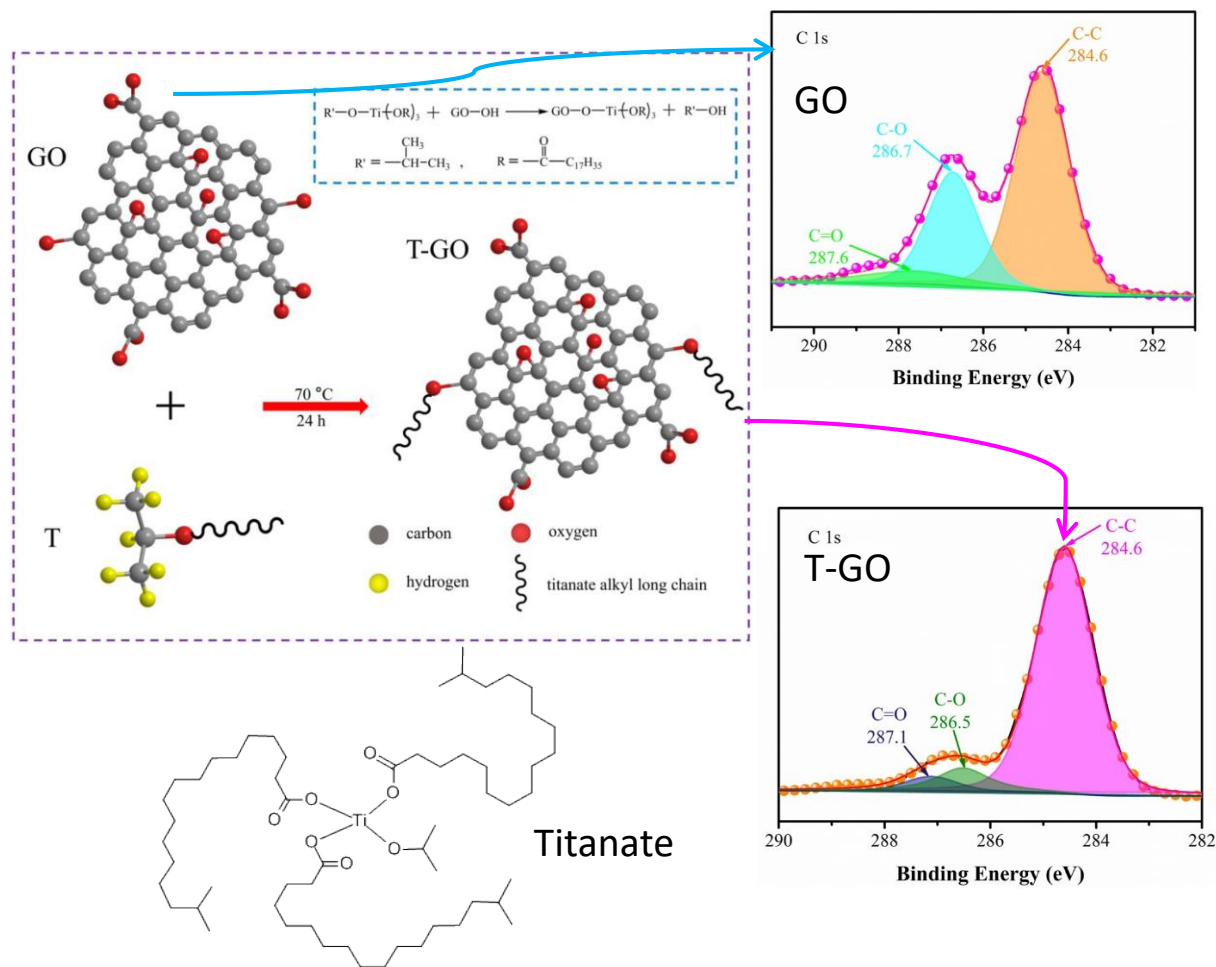


**Figure 7.** Covalent modification of graphene oxide with isopropyl triisostearyl titanate. Reproduced from <sup>64</sup> with permission of Elsevier.

### 3.4. Modification of biochar by ionic and nonionic surfactants

Biochar surface properties could be changed through modification with the surfactant layers. The ionic and non-ionic surfactant adsorbed on the solid surface influence the specific surface area, the content of acidic-basic functional groups, and the hydrophobic properties of these materials. Various mechanisms of surfactant molecule binding can be involved in such kinds of systems. The electrostatic interactions, hydrogen bonds, interactions between the  $\pi$ - $\pi$  electrons, bilayer formation, and hydrophobic interactions are associated with the adsorption of the surfactant, schematically presented in Figure 8.

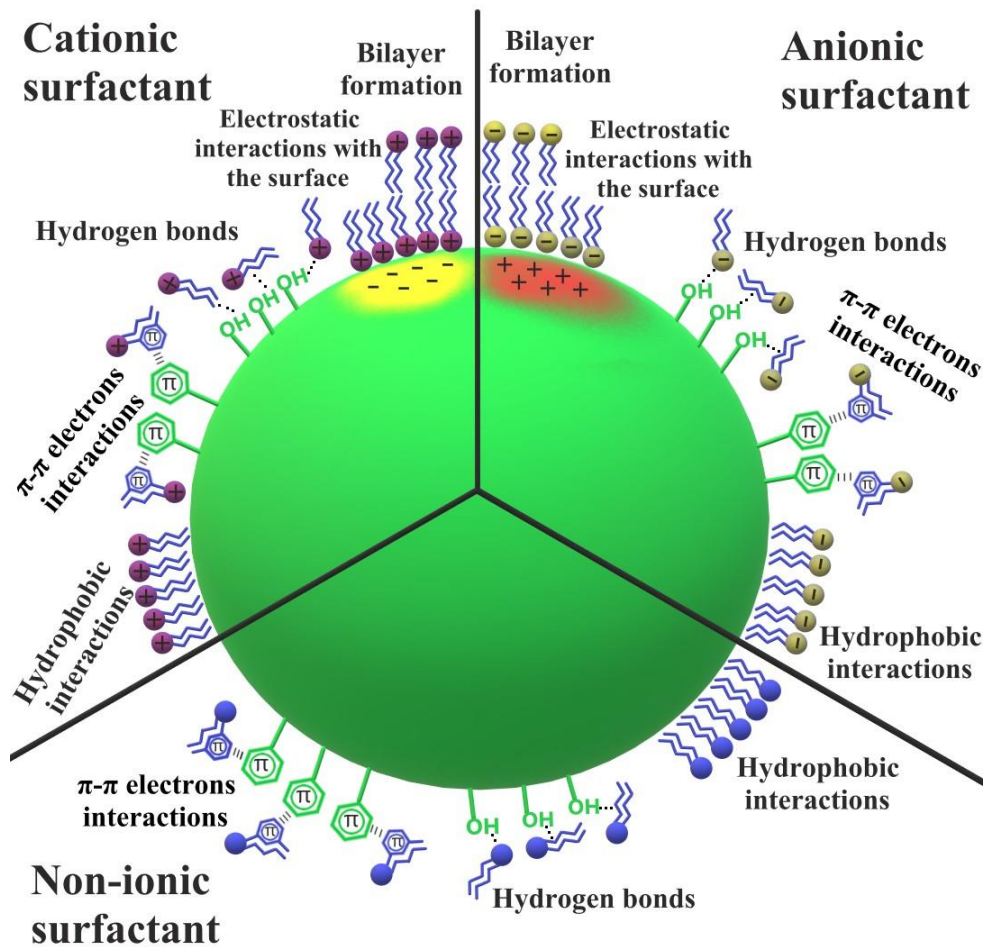


**Figure 8.** Possible adsorption mechanisms of surfactants with various ionic character on biochar surface.

These modifications with the surface active agents can both increase and decrease the biochar adsorption capacity, depending on the adsorbate and surfactant chemical character. The adsorption phenomenon could take place due to the all above-mentioned mechanisms. Moreover, the surfactant-adsorbate multilayer creation and the micelles formation have a positive effect on the adsorbed amounts of inorganic and organic substances (Figure 9).

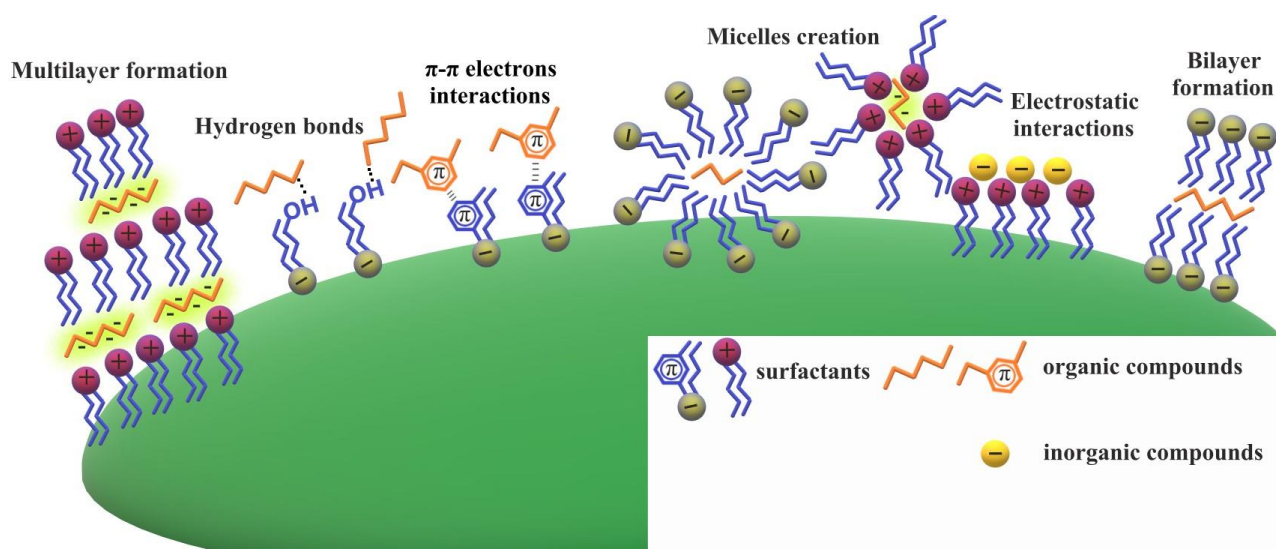


Figure 9. Possible mechanisms of organic and inorganic compounds adsorption on surfactant-modified biochar surface.

Biochar obtained from the *Populus alba* tree was modified with the cationic surfactant, cetyltrimethyl ammonium bromide (CTAB), and used for Cr(VI) adsorption. The obtained results proved that the surfactant modification affects the Cr(VI) adsorption favourably. The adsorbed amount increases on the modified biochar surface in comparison with the non-modified one independently of the adsorbent dose.<sup>65</sup> CTAB was also used for the biochar derived from the rice husk. The obtained results showed that due to the modification of the adsorbent, its surface charge change to be positive. The modified biochar was used for inorganic nitrogen fertilizers removal from the aqueous solution. The removal percentage increased by 13 % in the case of the modified adsorbent application in comparison to the non-modified material.<sup>66</sup>

The cationic CTAB modification was also performed in the case of the activated biochars obtained from the peanut shells and corncobs used for the anionic polymer-poly(acrylic acid) (PAA) adsorption. The surfactant modification favoured the increase of the polymer adsorption amount on both examined adsorbents. The poly(acrylic acid) removal from the aqueous solution is strongly related to its pH value, however, at all examined pH values (3, 6, 9), the anionic polymer is better adsorbed on the surface of the CTAB-modified activated biochar. In such a case the maximum PAA adsorbed amount was 68 mg/g.<sup>67</sup>

The CTAB-modified biochar obtained from the peanut shells and corncobs were likewise used for the Bisphenol A adsorption. The pyrolysis was performed at 300, 500 and 700 °C. It was found that the CTAB modification inhibits the Bisphenol A adsorption and this effect becomes stronger with the increasing pyrolysis temperature. It was also proved that the higher the surfactant concentration was applied, the smaller adsorbed amount of Bisphenol was found.<sup>68</sup>

The CTAB-modified coffee husk-activated biochar was used for the reactive dye removal from the aqueous solution. The reactive yellow 145 (RDY145) dye adsorbed amount was the largest on the surface of the

CTAB-modified activated biochar in comparison to two commercially available different non-modified activated carbons. The pH value has no significant effect on the RDY145 adsorbed amount. The Reactive Red 195 and Reactive Blue 222 dyes were also effectively separated from the aqueous system.<sup>69</sup> The other studies deal with the adsorption of Orange II (OII) and Methylene Blue (MB) dyes on the CTAB-modified biochar obtained from the cornstalk. Due to the adsorbent charge changing to positive (the non-modified biochar has a negative surface charge), the adsorbed amount of positively charged methylene blue decreases. In turn, the adsorbed amount of negatively charged OII increases compared to that observed for non-modified biochar. These effects are related to the electrostatic adsorption mechanism. The obtained maximum removal using the modified biochar was 40 % for methylene blue and 100 % for OII.<sup>70</sup>

The anionic surfactant, sodium dodecyl benzene sulfonate (SDBS) was used for the surface modification of the biochar obtained from the rice husk. The modified adsorbent was used for the inorganic nitrogen fertilizers removal from the aqueous solution. It was proved that the surfactant modification increases the removal efficiency by 2 % compared to the non-modified biochar.<sup>66</sup>

Sodium dodecyl sulfate (SDS) is an anionic surfactant which was used for modification of activated biochars obtained from peanut shells, corncobs, and peat. All above-mentioned adsorbents were used for the poly(acrylic acid) adsorption. The experiments indicated that the SDS modification effect on the PAA adsorbed amount depends largely on the adsorbent type and the solution pH value. On the surface of the activated biochars obtained from the peanut shells and corncobs, poly(acrylic acid) adsorption was inhibited at pH 9, however at pH 3 and 6 the surfactant modification affect the polymer adsorbed amount favourably. This is probably related to the PAA conformation change at different pH values. The maximum removal was 60 %.<sup>67</sup> Moreover the SDS modification reduced largely the PAA adsorbed amount at pH 4.5, 6 and 9 on the surface of activated biochar derived from the peat compared to the non-modified one. However, at pH 3, the modification did not affect significantly the polymer removal, which remained in the amount of over 90 %.<sup>71</sup>

The anionic SDBS surfactant was used for modification of the biochar derived from the peanut shells. The obtained biochar was used for the Bisphenol A adsorption. It was proved that the SDBS modification affects the Bisphenol A adsorbed amount negatively. The inhibition became stronger and stronger with the increasing surfactant concentration. The Bisphenol A adsorbed amount on the surface of the non-modified biochar was 100 mg/g and on the surface of SDBD-modified biochar 10 mg/g.<sup>68</sup>

The biochar obtained from the cassava peels was modified with the SDBS and SDS surfactants and used for Methylene Blue adsorption. It was proved that the SDBS-modified sample resulted in a larger number of surface active sites and increased the dye adsorbed amount. In the case of SDS, due to the changes of the adsorbent surface charge to negative, it had the favourable impact on the dye adsorbed amount increase.<sup>72, 73</sup> MB was also adsorbed on the surface of the SDS-modified biochar obtained

from the peanut shells. The adsorbent was modified with SDS of different concentrations. The obtained results showed that with the increasing surfactant concentration, the surface area accessible to adsorption increases. As a result, the Methylene Blue adsorbed amounts were considerably larger. The maximum adsorption capacity of the SDS-modified biochar as regards MB was 503 mg/g.<sup>74</sup>

The SDBS and SDS anionic surfactants were applied for the magnetic biochars derived from the corncobs and furfural residue modification. The obtained adsorbents were used for norfloxacin (an antibiotic with bactericidal action) adsorption. It was proved that the surfactant modification increased the norfloxacin adsorbed amount. The SBDS with a small concentration showed a larger impact on the antibiotic adsorption whereas SDS with higher concentrations was more effective.<sup>41</sup>

Magnetic biochars modified with the amphoteric surfactant - dodecyl dimethyl betaine (BS-12) were used for the phenanthrene adsorption. The adsorbed amount of phenanthrene BS-MC (a substance from the group of polycyclic aromatic hydrocarbons) decreased with the increasing BS-12 surface coating ratio. The change in the solution pH values caused no significant effects on the phenanthrene adsorption.<sup>75</sup>

Triton X-100 (2-{4-(2,4,4-trimethylpentan-2-yl)phenoxy}ethanol) belongs to the group of non-ionic surfactants. It was used for the activated biochar derived from the horsetail herb modification. The obtained adsorbent was successfully applied for the poly(acrylic acid) polymer and toxic Pb(II) heavy metal adsorption from the aqueous solutions. It was shown that the PAA adsorbed amounts decrease on the surface of the modified biochar compared to the non-modified one whereas the Pb(II) adsorption is more effective on the surface of the Triton X-100-modified adsorbent.<sup>76</sup> Poly(acrylic acid) was also adsorbed on the surface of the activated biochars obtained from the peanut shells and corncobs, modified with Triton X-100. The surfactant modification had a small impact on the PAA adsorbed amount. Moreover, the changes in the solution pH values (3, 6, 9) influenced the poly(acrylic acid) adsorbed amount more significantly compared with any adsorbent modifications with the surface active agent. The obtained maximum adsorbed amount of PAA on the Triton X-100-modified activated biochar was 55 mg/g.<sup>67</sup>

The biochars obtained from the peanut shells used for the Bisphenol A removal were modified with the non-ionic surfactant Tween 20 (polyoxyethylene (20) sorbitan monolaurate). Its effect on Bisphenol A adsorbed amount was similar to that caused by the ionic surfactants (CTAB, SDBS). The adsorbed amount decreased 10 times on the surface of the Tween 20-modified biochar in comparison to the non-modified one. The adsorption efficiency decreased with the increasing concentration of Tween 20.<sup>68</sup>

After the chemical activation, the biochars obtained from the eucalyptus sawdust were modified with the three different non-ionic surfactants: PEG 2000 (polyethylene glycol), Pluronic P-123 (poly(ethylene glycol)-*block*-poly(propylene glycol)-*block*-poly(ethylene glycol)) and Pluronic F-127 (2-{2-(2-hydroxyethoxy)propoxy}ethanol)) and used for the adsorption of metronidazole (an antibiotic used to treat infections with anaerobic microorganisms and mixed flora with anaerobes). All of the examined surfactants (dissolved in ethanol) affected the solid porous

structure. PEG 2000 and Pluronic P-123 increased the pore volume and its mean diameter whereas Pluronic F-127 enhanced only the pore size. All the above surfactants had an impact on metronidazole adsorption. The antibiotic exhibited the greatest affinity for the surface of the adsorbent modified with PEG 2000 (removal 100 %) whereas its adsorbed amount was the smallest on the surface of the Pluronic F-127-modified biochar (removal 80 %).<sup>77</sup>

Table 3 summarizes the experimental conditions for the design and salient features of surfactant-modified biochar specimens, whereas Figure 10 presents the possible applications of surfactant-modified biochars.

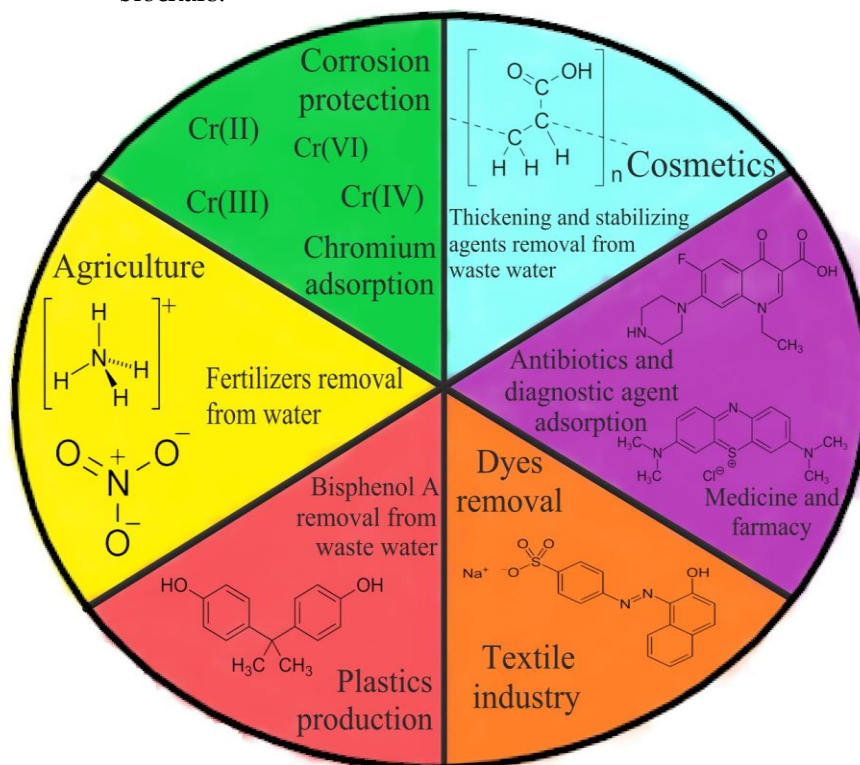


Figure 10. Applications of biochars modified by surfactants in various fields of human activity.

**Table 3.** Summary of inorganic and organic compounds adsorption on the surfactant-modified biochar surface.

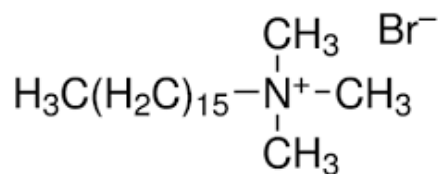
---

<b>Surfactant</b>	<b>Biomass used for biochar preparation</b>	<b>Surfactant immobilization conditions</b>	<b>Properties of modified biochar</b>	<b>Application</b>	<b>Reference</b>
-------------------	---	---	---	--------------------	------------------

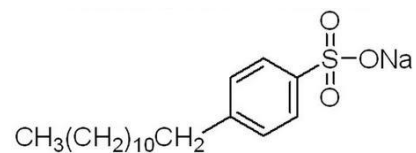
---



Cationic CTAB	<i>Populus alba</i>	Co: 22 mg/L Dried at 105 °C	-	Cr(VI)	65
	Rice husk	Co: 1457 mg/L Dried at 60 °C	Surface charge change to positive	Inorganic nitrogen fertilizers removal	66
	Peanut shells	Co: 100 mg/L	-	Poly(acrylic acid) adsorption	67
	Corncoobs	pH=3, 6, 9			
	Peanut shells	Co: 17-272 mg/L T: 25 °C pH: 6	-	Bisphenol A adsorption	68
	Coffee husk	Co: 2550 mg/L T: 30 °C Dried at 60 °C	Specific surface area decrease (from 750.1 to 557.4 m <sup>2</sup> /g) Pore volume decrease (from 0.3541 to 0.3192 cm <sup>3</sup> /g) Pore mean diameter increase (from 18.9 to 22.9 Å)	Reactive dyes removal	69
Cornstalks	Co: 10 mg/L Dried at 60 °C Neutral pH	Surface charge change to positive	Orange II and methylene blue adsorption	70	

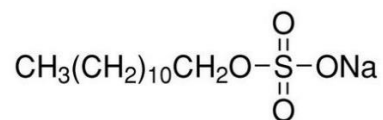


Anionic SDBS



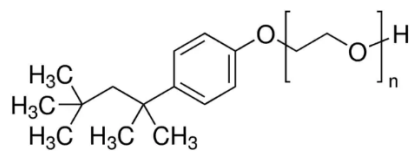
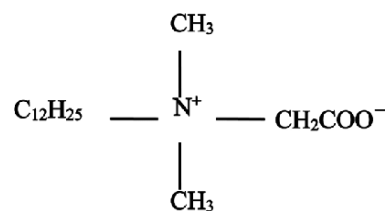
Rice husk	<p><math>C_0</math>: 437.5 mg/L</p> <p>Dried at 60 °C</p>	Surface charge change to negative	Inorganic nitrogen fertilizers removal	66
Peanut shells	<p><math>C_0</math>: 24.5-392 mg/L</p> <p>T: 25 °C</p> <p>pH: 6</p>	-	Bisphenol A adsorption	68
Cassava peels	<p><math>C_0</math>: 30-150 mg</p> <p>Dried at 110 °C</p>	More numerous surface active sites availability	Methylene blue adsorption	72
Corncob	$C_0$ : 61.25-3062.5 mg/L		Norfloxacin adsorption	41
Furfural residue	pH: 2-10			

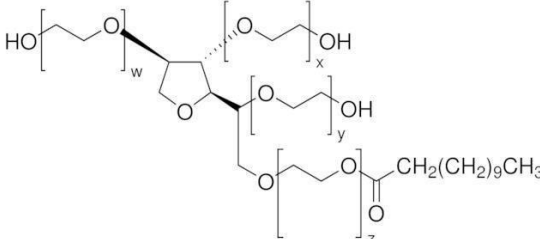
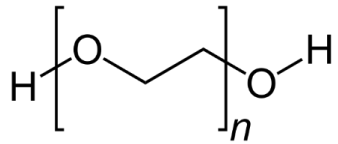
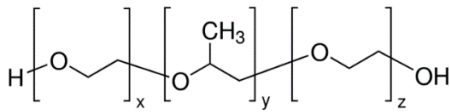
Anionic SDS

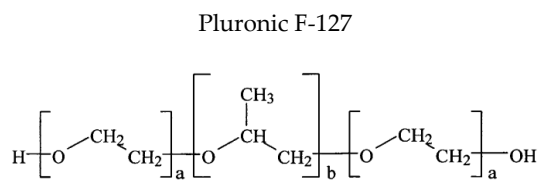


Peanut shells	$C_0$ : 100 mg/L		Poly(acrylic acid) adsorption	67
Corncobs	pH: 3, 6, 9			
Peat	<p><math>C_0</math>: 100 mg/L</p> <p>pH: 3, 4.5, 6, 9</p>		Poly(acrylic acid) adsorption	71
Cassava peels	<p><math>C_0</math>: 30-150 mg/L</p> <p>Dried at 110 °C</p>		Methylene blue adsorption	73

			Specific surface area increase (from 51.37 to 85.62 m <sup>2</sup> /g)		
	Peanut shells	Co: 6-30 mg/L Dried at 65 °C	Pore volume increase (from 0.232 to 0.283 cm <sup>3</sup> /g)	Methylene blue adsorption	74
			Pore mean diameter decrease (from 3.794 to 1.543 nm)		
	Corncob	Co: 61.25-3062.5 mg/L		Norfloxacin adsorption	41
	Furfural residue	pH: 2-10			
<hr/>					
Amphoteric BS-12					
			Modification 25-200 %		
				Phenanthrene adsorption	75
<hr/>					
Non-ionic Triton X-100					
	Horsetail herb	Co: 100 mg/L pH: 3		Poly(acrylic acid) and Pb(II) adsorption	76
	Peanut shells	Co: 100 mg/L		Poly(acrylic acid) adsorption	67
	Corncoobs	pH: 3, 6, 9			



Non-ionic Tween 20							
	Peanut shells	Co: 3.5-56 mg/L T: 25 °C pH: 6	-	Bisphenol A adsorption	68		
PEG2000							
	Eucalyptus sawdust	Surfactant dissolved in ethanol T: 60 °C Neutral pH	Specific surface area decrease (from 462 to 448 m <sup>2</sup> /g) Pore volume increase (from 0.309 to 0.392 cm <sup>3</sup> /g) Pore mean diameter increase (from 2.679 to 3.497 nm)	Metronidazole adsorption	77		
Pluronic P-123							
	Eucalyptus sawdust	Surfactant dissolved in ethanol T: 60 °C Neutral pH	Specific surface area decrease (from 462 to 436 m <sup>2</sup> /g) Pore volume increase (from 0.309 to 0.3586 cm <sup>3</sup> /g) Pore mean diameter increase (from 2.679 to 3.289 nm)	Metronidazole adsorption	77		



Eucalyptus sawdust

Surfactant dissolved in ethanol

T: 60 °C

Neutral pH

Specific surface area decrease

(from 462 to 221 m<sup>2</sup>/g)

Pore volume decrease  
(from 0.309 to 0.2465 cm<sup>3</sup>/g)

Pore mean diameter increase  
(from 2.679 to 4.466 nm)

Metronidazole adsorption

77

### 3.5. Surface arylation with diazonium salts

The chemistry of aryl diazonium salts dates back to the mid-1800s<sup>78</sup> and was at the origin of the industrial production of azo dyes.<sup>79</sup> It is also explored in numerous organic synthesis reactions.<sup>80</sup> Only since 1992 it became world-wide applied to modify materials surfaces, particularly carbon allotropes.<sup>40, 81</sup> This approach is alluring because of its commercially abundant comprising aromatic amines with various functional groups, as diazonium precursors.

A general pathway for the modification of carbon materials is depicted in Figure 11. Mostly, the *ex-situ* or *in-situ* generated diazonium salt reacts in aqueous or organic solvents in order to provide radicals that attack the surface, or the diazonium forms diazoether interfacial bond, followed by release of dinitrogen and formation of C-O-C interface. Example is given for carbon surface bearing surface functional groups.

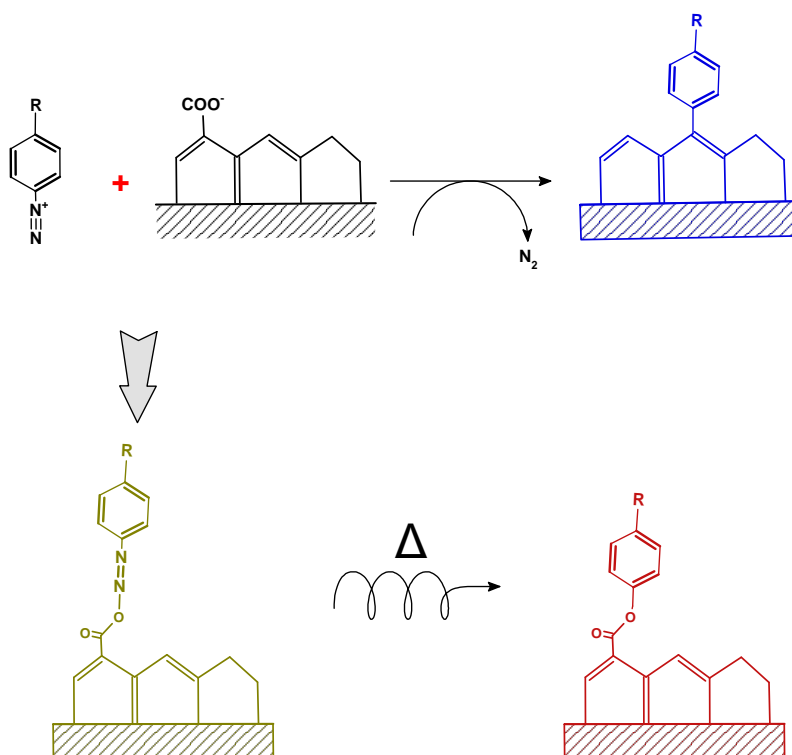


**Figure 11.** Schematic illustration of the modification of a graphitic surface with aryl diazonium salts.

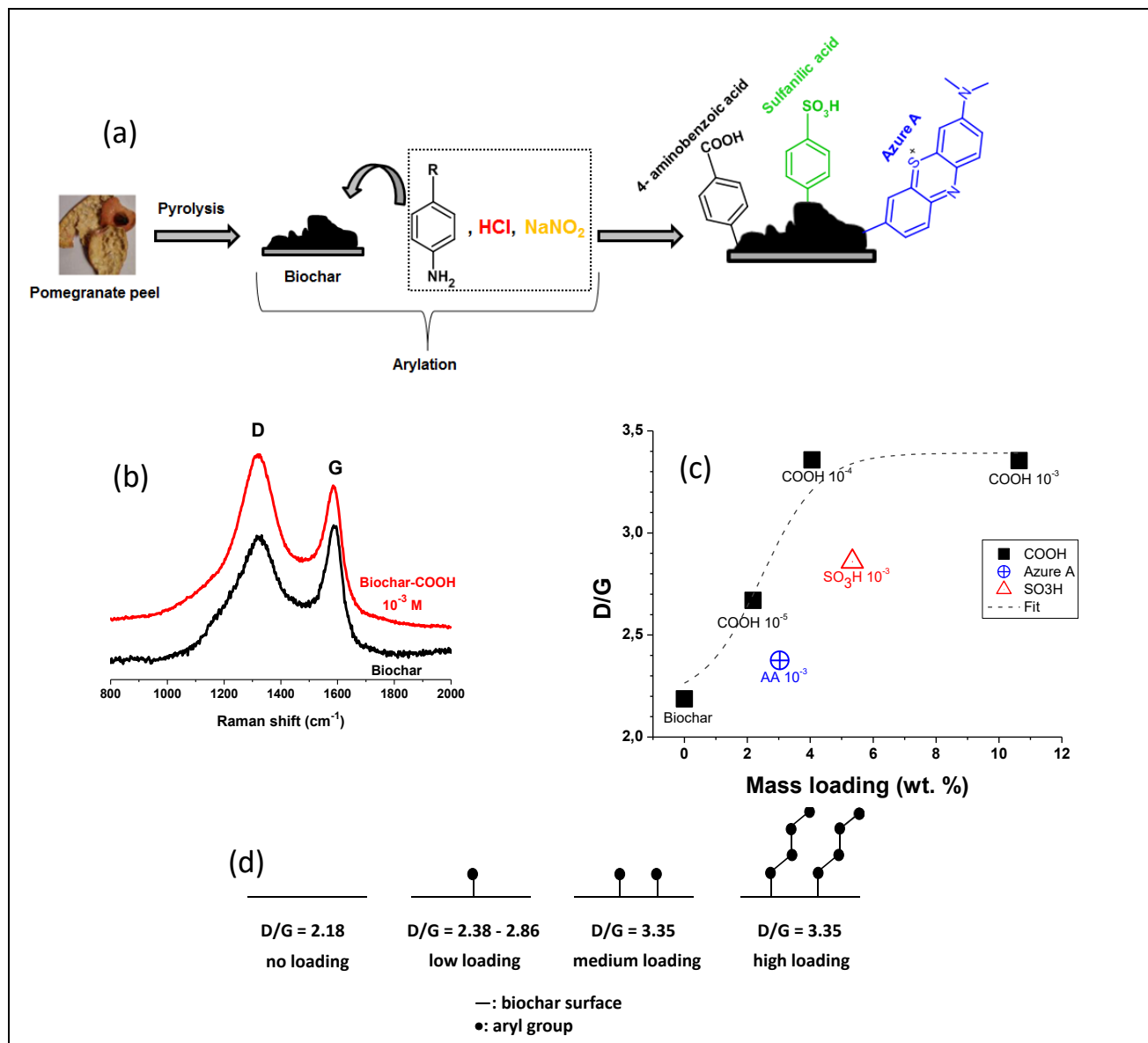
Biochar is among these functionalized carbons and is thus prone to arylation with diazonium salts. The grafted aryl groups display scaffolds to link moieties through specific reactions as they possess suitable functional groups. They comprise amide coupling, coordination bonding and click chemistry.<sup>55</sup> The surface-aryl bond is usually strong owing to its covalent nature, therefore ensuring remarkable mechanical properties of polymers reinforced with arylated fillers, or strong adhesive bonding of polymers to

25 arylated surfaces. One can also take advantage of the strong arylation of carbonaceous  
26 supports to anchor bimetallic nanocatalysts, with excellent dispersion and narrow size  
27 distribution for nitrate electroreduction application.<sup>82</sup>

28  
29 The arylation of carbon allotropes including fullerene, graphene, and carbon nanotubes  
30 with diazonium salts showed enhanced properties and performances in several domains  
31 such as electrocatalysis, sensing, and optics.<sup>55</sup> However, these precursors are expensive  
32 with limited large-scale applications. Alternatively, the obtained biochar from agrowaste  
33 pyrolysis can provide a highly porous matrix compared to the initial lignocellulosic  
34 materials.<sup>83</sup> Biochar can be treated with acids or alkalis to provide a higher surface area  
35 with enhanced porous structure. Apple leave-derived char was activated through  
36 various processes. This work study was concerned with investigating the impact of acid  
37 and thermal treatments on the physico-chemical properties of the resulting biochar. The  
38 latter was capable of abstracting the organic pollutants from water.<sup>84</sup> Several Raman  
39 spectra for carbonaceous matters seem to be complex. It may be referred to the as  
40 complicated structure they possess. The simplest spectrum is for graphite because of the  
41 uniformity of its formation showing planar and stratified laminates. Relative  
42 deformations may arise in this structure expressing a weak D band with a directly  
43 proportional intensity to the extent of disorders in this structure. Khalil et al.<sup>85</sup>  
44 investigated fundamental variations in the D/G peak intensity ratio on going from the  
45 pristine biochar derived from pomegranate peels when compared to different arylated  
46 biochar samples; namely Biochar-COOH, biochar-SO<sub>3</sub>H, and biochar-Azure A. The  
47 results expressed that D/G peak ratio grows with arylation without depending on the  
48 kind of diazonium compound. The intensity of Raman D/G peaks was correlated to the  
49 elementary concentration of the employed diazonium salts. Figure 12a depicts the  
50 general route for arylation of pomegranate biochar with in situ generated three  
51 diazonium salts. Figure 12b compares the Raman bands of pristine and arylated biochar;  
52 the D/G intensity ratio increases upon treatment of diazonium salts, which is a sign of  
53 true covalent modification resulting from arylation. Figure 12c plots D/G ratio as a  
54 function of the grafting extent determined by TGA. Interestingly, for similar high initial  
55 concentrations, Azure A induces marginal change in D/G intensity ratio due to steric  
56 hindrance. Figure 12d schematically illustrates the gradual change in the grafting density  
57 of aryl groups at the surface. High initial concentration is likely to result in  
58 oligomerization of the aryl groups,<sup>56,86</sup> hence the tendency of the D/G intensity ratio to  
59 reach a plateau value. Indeed, chemical grafting reactions no longer affect the carbon  
60 allotrope support, but the organic layer, previously attached.<sup>87</sup>

25  
26  
27  
28  
29  
30  
31  
32  
33  
34  
35  
36  
37  
38  
39  
40  
41  
42  
43  
44  
45  
46  
47  
48  
49  
50  
51  
52  
53  
54  
55  
56  
57  
58  
59  
60  
61

62



63 **Figure 12.** Arylation of pomegranate biochar: (a) modification with in situ generated diazonium salts, (b) Raman  
 64 spectra of biochar and carboxyphenyl-modified biochar using a  $10^{-3} M$  aromatic amine solution, (c) plot of D/G vs  
 65 mass loading (wt.%) for different biochar samples, and (d) schematic illustration of stepwise growth of oligoaryl  
 66 chains and their effect on D/G peak area ratio. Reprinted from<sup>85</sup> with permission of Springer Nature.

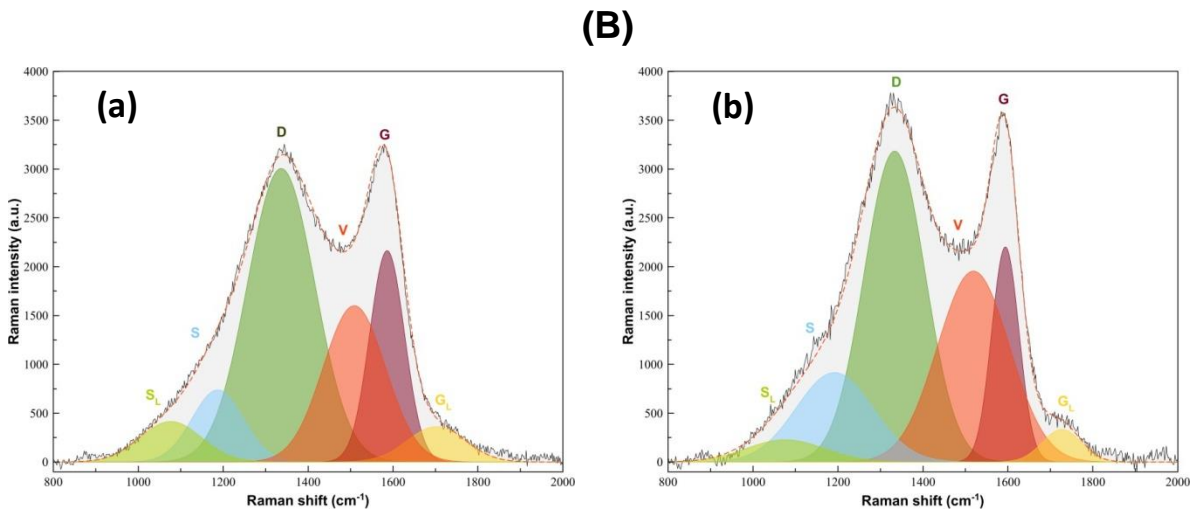
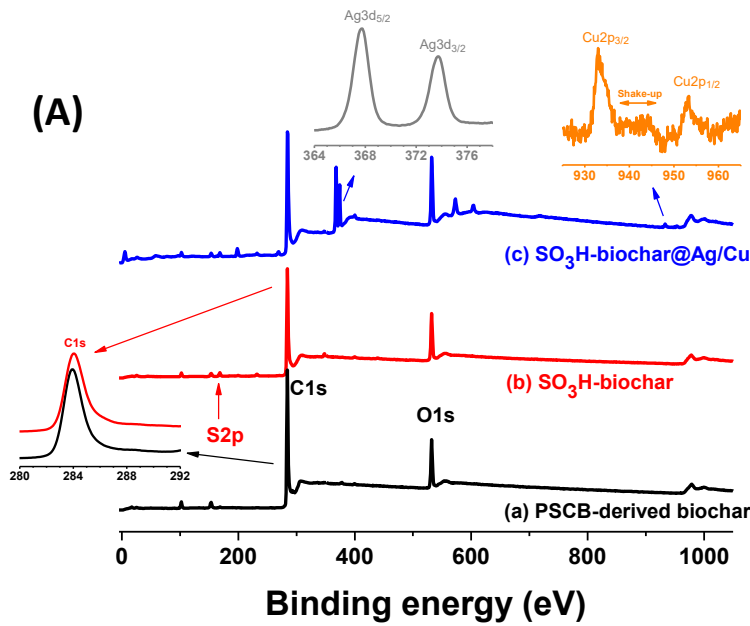
67

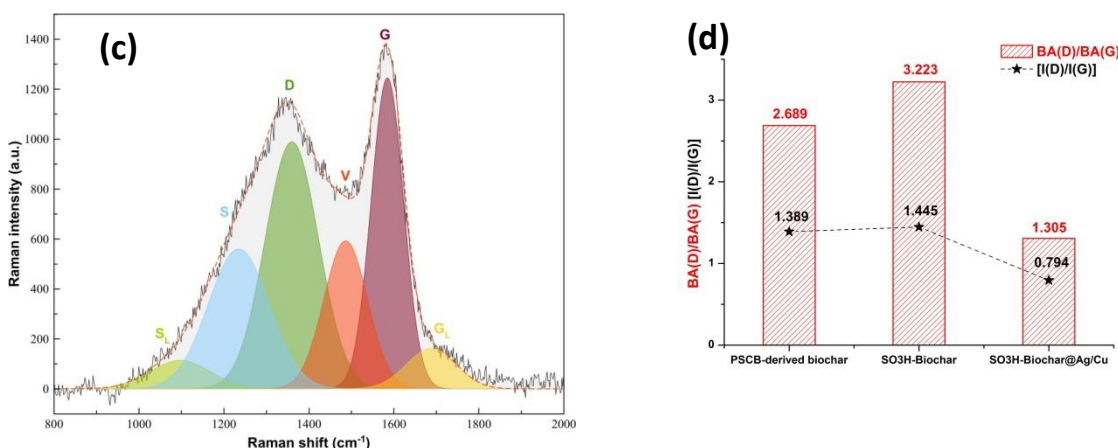
68 Snoussi et al.<sup>88</sup> prepared biochar from the pyrolysis of the pulp of sugarcane pulp  
 69 bagasse (PSCB) at  $500\text{ }^{\circ}C$ , and modified it with sulfanilic acid-based, in situ-generated  
 70 diazonium salts. AgCu bimetallic nanocatalyst was loaded by in situ reduction of the  
 71 silver and copper nitrate-impregnated arylated biochar (SO<sub>3</sub>H-Biochar), using  
 72 phytochemicals extracted from the biomass. Sulfonation and deposition of the bimetallic  
 73 AgCu nanocatalysts were probed by XPS (Figure 13A). Raman spectra (Figure 13B) curve  
 74 fitting permitted to determine D and G band area and height. This curve-fitting  
 75 permitted to show of deformations in the carbon lattice resulting from the arylation  
 76 process with some disorders when compared to the pristine biochar (Figure 13Ba-b). A



77  
78  
79  
80  
81  
82  
83

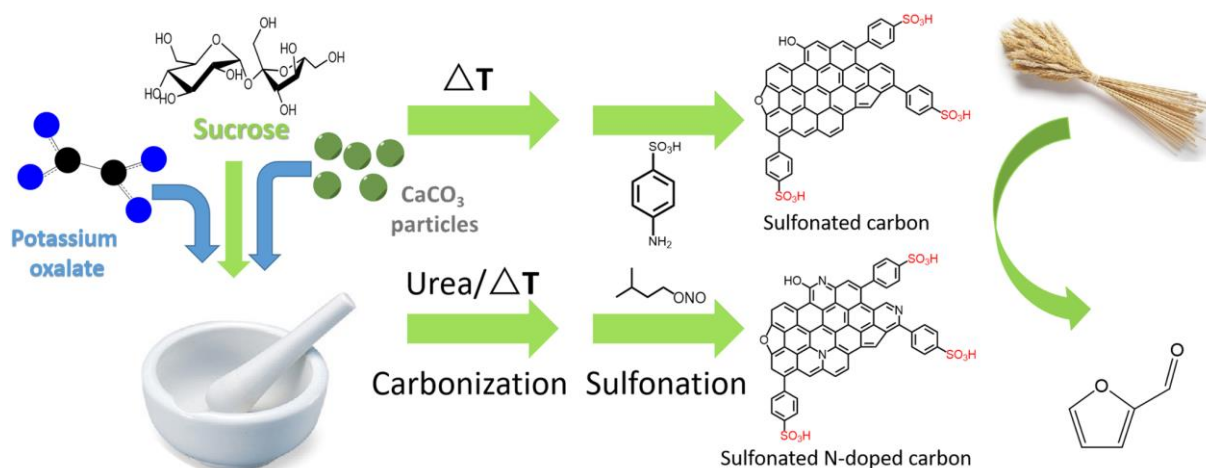
noticeable increase in biochar defects can be referred to the surface arylation (Figure 13Bb), whereas with a minor effect resulting in a slightly higher D/G band intensity ratio. However, upon metal deposition, a significant relative increase in the G band area or height and thus a decrease in D/G band area or peak height intensity ratio suggested an increase in the graphitization, resulting in boosting the catalytic efficiency.





84 **Figure 13.** (A) XPS analysis of sugarcane bagasse biochar and related sulfonated biochar and biochar@Ag/Cu. (B)  
 85 Curve fitting of Raman spectra of (a) sugarcane pulp bagasse (PSCB)-derived biochar, (b) SO<sub>3</sub>H-Biochar, (c) SO<sub>3</sub>H-  
 86 Biochar@Ag/Cu, and (d) the evolution of BA(D)/BA (G) and I(D)/I(G) ratios based on the curve fitting calculations  
 87

88 Arylation of the activated carbon with 4-sulfobenzene diazonium chloride was carried  
 89 out for synthesizing 4-sulfophenyl activated carbon to act as an efficient catalyst.  
 90 Changing the conditions of the reaction provided an arylated activated carbon with  
 91 sulfanilic acid possessing numerous acid sites. The used catalyst was recovered easily  
 92 upon utilizing it in esterification reactions of some fatty acids.<sup>89</sup> Bamboo activated carbon  
 93 was arylated by sulfanilic acid to produce heterogeneous catalysts. The prepared  
 94 arylated catalysts showed high activity in esterifying oleic acid with alcohol. The  
 95 microstructure shrinkage may lead to deactivation of the heterogeneous acid catalyst.  
 96 Meanwhile, the regenerated catalyst can be used providing an efficiency over 90%.<sup>90</sup>  
 97 Sulfonated sucrose-based and N-doped activated carbon were prepared using N-source,  
 98 pore-forming, and sulfonating agent to act as catalysts. They were then employed in  
 99 producing furfural from wheat straw (Figure 14). One of these modified catalysts showed  
 100 acceptable recyclability. The aromatic sulfanilic acid groups were successfully grafted  
 101 onto the activated carbons via a simple sulfonation procedure.<sup>91</sup>  
 102  
 103

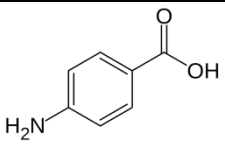
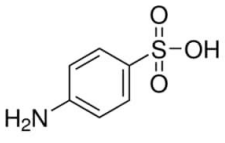
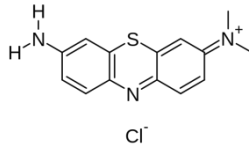


105 **Figure 14.** Schematic illustration of the preparation of sulfonated biochar as a catalyst of furfural production from  
106 wheat straw. Reproduced from [91] with permission of Elsevier.

107  
108 In another study, sulfonated bio-carbon samples were prepared via partial carbonization  
109 of biomass-based substrates with sulfuric acid or diazonium salt. The performance of the  
110 catalysts relied upon the concentration of sulfonic acid groups.<sup>92</sup> Sulfonated carbon  
111 materials are covalently functionalized with sulfonic acid groups. They show promising  
112 efficiency and selectivity, surpassing traditional acid catalysts. The eminent performance  
113 of sulfonated carbonaceous substrates may be correlated to their distinctive  
114 topographical features, enhancing catalysis and selective adsorption.<sup>93</sup> Amino-arene-  
115 sulfonic acid was used to sulfonate biochar for producing a hydrophobic sulfonic acid  
116 functional biochar in a one-pot diazo-reduction process. The length of the arene chain  
117 and the grafting magnitude of arenesulfonic acid are substantial factors in monitoring the  
118 hydrophobicity of the functionalized biochar catalysts. The latters have a large surface  
119 area with an appropriate pore size distribution. This modified biochar supplies an active  
120 catalyst in many transformation reactions. These catalysts showed catalytic efficiencies in  
121 alkylating 2-methylfuran with cyclopentanone in biofuel production.<sup>94</sup>

122  
123 Table 4 gathers the salient features of some biochar samples arylated under diverse  
124 conditions and for various applications such as the catalysed transformation of furfural,  
125 or esterification reaction. Arylation is certainly of interest, but if it is conducted with a  
126 high initial diazonium concentration, it will lead to sharp decrease of the specific surface  
127 area, and the porous volume. Arylation with in situ generated diazonium salts requires  
128 strong acidic medium, *i.e.* 25-37% HCl. This could favour the formation of a porous  
129 structure.

**Table 4. Surface treatment of biochar with aryl diazonium salts**

Coupling agent	Biomass	Surface treatment conditions	Properties of engineered biochar	Potential application	References
	Pomegranate peel	Reaction with in situ generated diazonium salt, in 37% HCl, amine:NaNO <sub>2</sub> = 1:1; final diazonium concentration=10 <sup>-5</sup> -10 <sup>-3</sup> M	Controlled arylation, mass loading = 2.2-10.6 wt/wt%, D/G=2.7-3.4 (peak area ratio).	NA, potential heavy metal removal,	85
	Sugarcane bagasse	Reaction of 300 mg biochar with in situ generated diazonium salt, in 37% HCl, amine:NaNO <sub>2</sub> = 1:1 (6 mmol:6 mmol);	Arylation yields the grafting of 2 SO <sub>3</sub> per 100 biochar carbon atoms. D/G=1.39 for biochar and 1.45 for biochar-SO <sub>3</sub> H. Arylation with in situ generated diazonium in concentrated HCl induces channel formation within the biochar.	In situ deposition of Ag(I) and Cu(II) ions, followed by reduction using sugarcane bagasse extract.	88
	Pomegranate peel	Reaction with in situ generated diazonium salt, in 37% HCl, amine:NaNO <sub>2</sub> = 1:1; final diazonium concentration=10 <sup>-3</sup> M	Mass loading = 5.3%, D/G=2.9 (peak area ratio)	NA, potential heavy metal removal	85
	Bamboo	Sulfanilic acid/Biochar molar ratio= 0.1-1.5, in 25% HCl, at 30-80 °C, for 2-60 min.	Total acid density=1.69 mmol/g. SSA decreased from 919 to 225 m <sup>2</sup> /g upon arylation.	Acid catalyst. Up to 96% catalyzed esterification of oleic acid with ethanol.	90
	Sucrose-K <sub>2</sub> C <sub>2</sub> O <sub>4</sub> •H <sub>2</sub> O-CaCO <sub>3</sub> -Urea (1-1-1-0 or 1-1-1-0.5 wt.fractions)	Biochar prepared at 600-800 °C without urea, and at 750 °C in the presence of urea. 1g biochar mixed with 4 g sulfanilic acid and 2 g isoamyl nitrite, in 150 mL DIW. Arylation at 80 °C overnight.	Drastic reduction of SSA from 1422 to 190 m <sup>2</sup> /g for biochar prepared at 800 °C, and from 1658 to 30 m <sup>2</sup> for biochar-urea and sulfonated biochar-urea. Sulfur content: 0.08 to 2.29 mmol/g. With urea, very high arylation D/G increased with arylation.	Catalytic furfural production from wheat straw.	91
	Pomegranate peel	Reaction with in situ generated diazonium salt, in 37% HCl, amine:NaNO <sub>2</sub> = 1:1; final diazonium concentration=10 <sup>-3</sup> M	Mass loading = 5.3%, D/G=2.9 (peak area ratio)	NA, potential radical polymerization photoinitiation	85

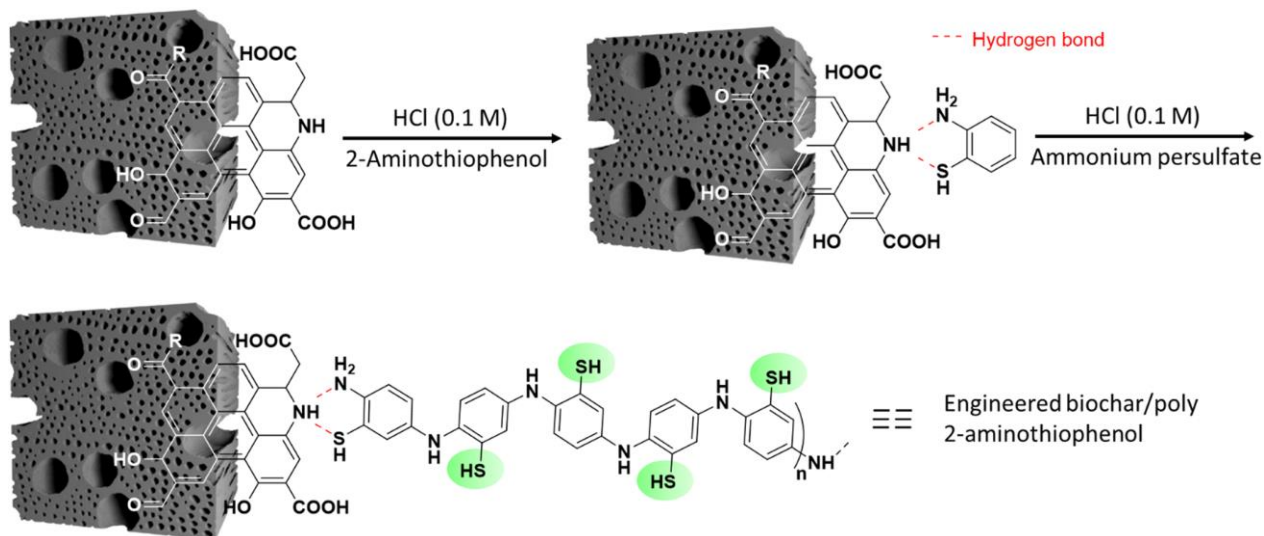
APTES: aminopropyl triethoxysilane; DIW: de-ionized water; SSA: specific surface area

### 3.6. Surface-modified biochar with nitrogen-based compounds

Owing to the versatility of  $sp^2$  carbon surface, and the availability of highly interacting functional groups, biochar is prone to molecular and macromolecular post-functionalization with aminated compounds. Doping biochar with nitrogen-containing compounds during pyrolysis or hydrothermal treatment of the biomass is out of scope and the reader is referred to selected articles on the topic.<sup>95-97</sup> Similarly, strong activation with nitric acid to provide surface amino groups is covered but not with a dedicated section; as an example see for example the work of Bamdad *et al.*<sup>98</sup>

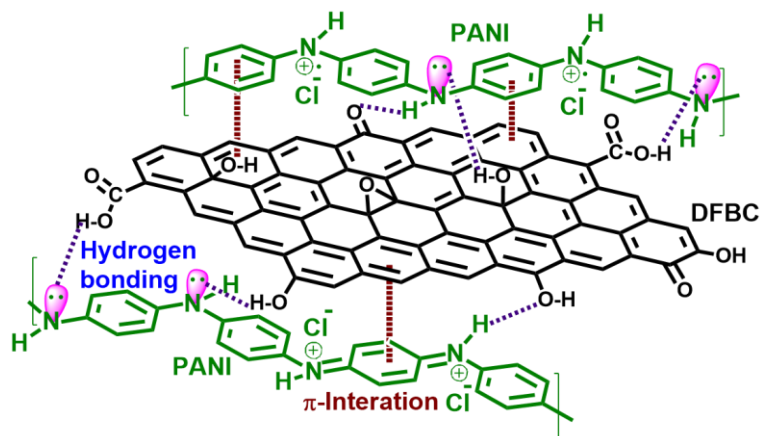
Modification can proceed with molecular coupling agent, or with adsorption of a monomer that is subjected to polymerization.

Two major nitrogen-containing compounds have been employed to modify the surface of biochar: aniline and 2-aminothiophenol-related compounds, and polyethyleneimine (PEI). The aniline derivatives are usually subjected to in situ oxidative polymerization in the presence of biochar. Surface-confined polymerization proceeds with the adsorption of the aniline derivative, most probably driven by biochar-COOH...H<sub>2</sub>N-C<sub>6</sub>H<sub>4</sub>-R hydrogen bonding. For example 2-aminothiophenol can be adsorbed on the surface of biochar and subjected to oxidative polymerization using ammonium persulfate to yield poly(2-aminothiophenol)-coated biochar particles (Figure 15).<sup>99</sup> Note that, in Figure 15, hydrogen bonds are shown for N...N interactions; in our fair opinion hydrogen bonds occur between NH<sub>2</sub> from the monomer and the COOH and/or OH from the biochar surface. Indeed, Lewis acid-base interactions, or more particularly hydrogen bonds are maximized for COOH-NH<sub>2</sub> rather than NH<sub>2</sub>-NH<sub>2</sub> interactions.<sup>100</sup> The biochar composite was tested for the uptake of Hg and As from wastewater and was found to remove over twice as much contaminants, at pH 9, compared to the untreated biochar. Adsorption levelled off at ~32 and 119 mg/g As(III) and Pb(II), respectively. These values are much higher than those recorded with unmodified biochar (14 and 47 mg/g for AS(III) and Pb(II), respectively). At this stage, it is essential to note that despite drastic two-fold decrease in the specific surface area of the engineered biochar owing to the polymer coating (118 and 59 m<sup>2</sup>/g for engineered and pristine biochar, respectively), removal of As(III) and Pb(II) remained high.



171 **Figure 15.** Schematic illustration of the route to engineered biochar/poly(2-aminothiophenol) adsorbent via in situ  
 172 oxidative polymerization of 2-aminothiophenol. Reproduced from<sup>99</sup> with permission of Elsevier.

174 Aniline is a much more investigated monomer to provide composites of biochar and  
 175 polyaniline (PANI). It can be synthesized in the presence of biochar and remains glued to  
 176 the latter via hydrogen bonds (Figure 16).



179 **Figure 16.** Biochar-PANI composite chemical structure. Dotted lines indicate hydrogen  
 180 and p-p bonds between biochar and the PANI deposit. Reproduced from<sup>101</sup> with  
 181 permission of Elsevier.

183 Douglas fir biochar was prepared by fast pyrolysis at 900-1000 °C and served for the in  
 184 situ deposition of PANI by oxidative polymerization.<sup>101</sup> 1g biochar-PANI composite  
 185 removed 150 mg Cr(VI) and 72 mg nitrates, at pH 2 and 6, respectively, much more than

186 the pristine biochar. PANI provides nitrogen-based anchoring sites for Cr(VI) and  
187 hydrogen bonding acceptor from biochar OH and COOH groups.

188 Magnetic biochar-PANI composites were prepared by wet impregnation of durian rind  
189 powder with three iron precursors, followed by pyrolysis at 800 °C. The resulting  
190 magnetic biochars were further coated with PANI via in situ oxidative polymerization of  
191 aniline using ammonium persulfate, in an acidic medium (1 M HCl), at 0-5 °C. The  
192 highest specific surface was 855 m<sup>2</sup>/g. The magnetic biochar prepared using FeCl<sub>3</sub>·6H<sub>2</sub>O  
193 precursor and topped with PANI was used as supercapacitor; it exhibited a specific  
194 capacitance of 615 F/g at 10 mV/s and an energy density of 76.9 Wh/kg.<sup>102</sup>

195 Magnetic banana stem biochar was prepared in situ deposition of magnetite after the  
196 carbonization process of the biomass at 500 °C. PANI was prepared by in situ  
197 polymerization to yield a supercapacitor composite material that has a specific  
198 capacitance  $C_s = 315.7 \text{ Fg}^{-1}$ , higher than that of the magnetic biochar without any PANI  
199 ( $C_s = 234.8 \text{ Fg}^{-1}$ ).<sup>103</sup>

200 Tobacco biochar was fabricated, treated with phosphoric acid and mixed with PANI,  
201 then Ag<sub>3</sub>PO<sub>4</sub> was synthesized in situ. The final Biochar/PANI/Ag<sub>3</sub>PO<sub>4</sub> was employed as  
202 a photocatalyst to degrade triclosan.<sup>104</sup> The rationale for making this ternary composite  
203 lies in the synergy between (i) the excellent photocatalytic properties of Ag<sub>3</sub>PO<sub>4</sub>, (ii) the  
204 electronic conductivity of biochar that favours rapid transfer of photogenerated electron  
205 (e<sup>-</sup>) of Ag<sub>3</sub>PO<sub>4</sub>, and (iii) PANI, a promoter of the transfer and separation of  
206 photogenerated hole-electron pairs (h<sup>+</sup>-e<sup>-</sup>), as well as an inhibitor of the photo-corrosion  
207 and oxidation of Ag<sub>3</sub>PO<sub>4</sub>. The composite catalysed the degradation of triclosan at a rate of  
208 85%, within 10 min.

209 Another type of biochar/polymer composites can be prepared by mixing biochar with  
210 PEI, using methanol or ethanol.<sup>105-109</sup> Electrostatic interaction between the protonated  
211 amino groups from the biochar and the carboxylate groups from biochar can take place.  
212 Also, strong hydrogen bonds are expected. Covalent grafting of PEI could be achieved  
213 using glutaraldehyde<sup>43, 110</sup> or EDTA dianhydride.<sup>106</sup> For example, the frequently  
214 employed glutaraldehyde is a good coupling agent as it reacts with OH functional  
215 groups<sup>111</sup> from biochar surface and the NH/NH<sub>2</sub> groups from PEI. An example of  
216 composite is illustrated in Figure 17 showing the fabrication of magnetic biochar-PEI  
217 nanocomposite employed for the removal of Cr(VI).  
218



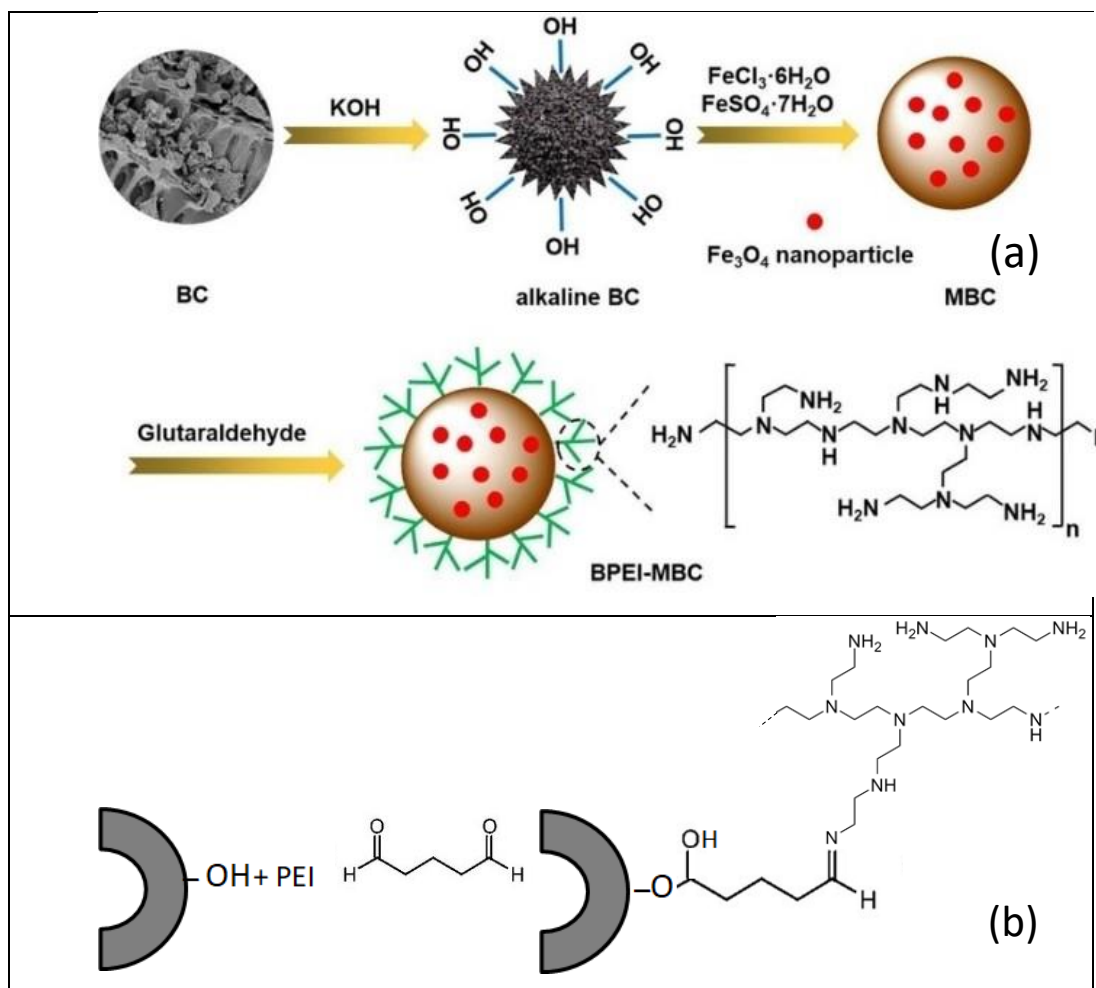


**Figure 17.** Schematic illustration of the fabrication of magnetic coconut shell biochar and its graft modification with PEI (a). Use of glutaraldehyde for coupling PEI to the underlying biochar (b). Figure 17a reproduced from with permission of Wiley & Sons.

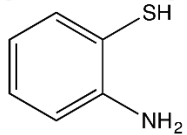
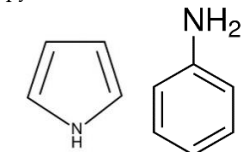
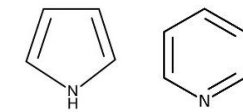
As a few examples of the performance of PEI-modified biochar materials, PEI-modified pine needles biochar permitted to adsorb 294 mg/g Congo Red, almost 10-fold the adsorption capacity of the pristine biochar (30.8 mg/g).<sup>112</sup>

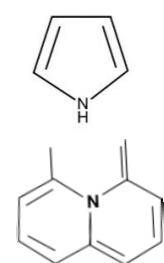
PEI-modified biochar was employed for detoxification of Cr(VI); it was found to remove 435.7 mg per g of biochar, nearly 20 times higher than 23.1 mg/g for pristine biochar.<sup>105</sup>

Table 5 reports experimental conditions, properties and applications of shortlisted biochars modified with nitrogen-containing molecules and macromolecules.

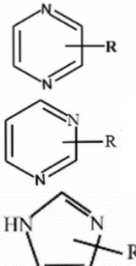


**Table 5.** Surface treatment of biochar with nitrogen-based compounds.

Coupling agent	Biomass	Surface treatment conditions	Properties of engineered biochar	Potential application	References
poly 2-aminothiophenol 	Date leaves	Reaction of 1000 mg date leaves biochar with in 2-aminothiophenol (0.5 mL), in 0.1 M HCl, 20 mL of a solution (0.1%) of ammonium persulfate.	SSA 59.02 m <sup>2</sup> /g, Average pore diameter 20.16 nm	Removal of arsenic and mercury ions from wastewater	99
pyrrole/aniline 	Forestry waste	Co-polymerization of polypyrrole/polyaniline on ferrate modified biochar. pyrrole/aniline (Volume ratios = 0:1 (0, 1 mL)- 1:0 (1, 0 mL) and 1 g CTAB were added into the above solution with HCl of 1 mol/L.	SSA 56.97 m <sup>2</sup> /g Pore-size distributions 17.98 nm	Adsorption of hexavalent chromium in water	113
pyrrolic- and pyridine-like N 	Birch tree	Birch trees/H <sub>3</sub> PO <sub>4</sub> (50 wt. %) / melamine weight ratio of 1:4:3 at 800 °C, for 1 h.	SSA dominated by mesopores (86.4 %), nitrogen functional groups with 5.4 % of N in its structure D/G=2.0.	Adsorption of acid red 18 dye.	114
pyrrolic N and graphitize N	Pomelo peel	Reaction with one-pot pyrolysis, Pomelo peel	Specific surface area 738 m <sup>2</sup> /g, nitrogen content 13.54 at%.	Removal of sulfamethoxazole	115



		powder, NaHCO <sub>3</sub> and melamine at a mass ratio of 1:3:4, 600-900 °C	D/G=0.96		
	Rice husk	Rice husk: urea mass ratio =1:3, sonicated for 1 h, pyrolyzed at 800 °C	N-atom content= 8.11%, D/G= 1.095. Nitrogen doping decreased the number of defects in the biochar.	Catalytic degradation of dimethomorph	116
	Pistachio shells	10g of pistachio shell as the carbon source, 2g of melamine as the nitrogen source, and 5g of NaHCO <sub>3</sub> /K <sub>2</sub> CO <sub>3</sub> as the activator.	SSA increased by about 1000 m <sup>2</sup> g <sup>-1</sup> after N-doping, the surface N content increased by more than 3 %, and hydrophilicity and polarity declined.	Selective adsorption of toluene under humid conditions	117
the formation of abundant N-containing functionalities in the form of C-N, C= N and N-H in C-N polymer structures.	Melon seed shell	Melon seed shell/ melamine Weight ratio= 1:1, in solvent (water and CH <sub>3</sub> CH <sub>2</sub> OH with a mass ratio of 1: 1), Dried and pyrolyzed at 400 °C.	D/G=0.71 (peak area ratio), formation of mesopores structure, average pore size of 12.6 nm, melamine or its derivatives reacted with the C= O functionality on the biochar, forming the C-N, C=N and N-H bond on the biochar. Biochar became hydrophilic after introducing nitrogen species	Photocatalytic production of hydrogen	118
C-N, amino groups	Camellia oleifera shells	Pretreating biomass with (NH <sub>4</sub> ) <sub>2</sub> S <sub>2</sub> O <sub>8</sub> 50 g of the Camellia oleifera shells powder was added to 100 mL of ammonium persulfate (1 mol L <sup>-1</sup> ) until dry, and then placed into a N <sub>2</sub> atmosphere for pyrolysis at 700 °C.	SSA increased from 134.9 m <sup>2</sup> g <sup>-1</sup> to 739.9 m <sup>2</sup> g <sup>-1</sup> , and the pore volume also increased from 0.301 cm <sup>3</sup> g <sup>-1</sup> to 0.588 cm <sup>3</sup> g <sup>-1</sup> after introduce N-containing groups, pretreatment with (NH <sub>4</sub> ) <sub>2</sub> S <sub>2</sub> O <sub>8</sub> introduce various polar nitrogen-containing and sulfur-containing functional groups into biochar.	The adsorption capacity for Cu(II) and tetracycline.	119

pyridinic-N (N-6), pyrrole/pyridine-N (N-5), and quaternary-N (N-Q)	coconut shell	Coconut shell/ urea ( Mass ratio of 1:1) by the thermal activation at 873 K for 2 h, and the medium temperature ionic liquid of molten alkali KOH (85% purity, the mass ratio to the intermediate material was 1.5:1)	SSA increased from 594.8 to 1711.4 m <sup>2</sup> g <sup>-1</sup> , total pore volume increased from 0.31 to 0.80 cm <sup>3</sup> /g, mean pore size after nitrogen doping	the capacity of CO <sub>2</sub> adsorption can be up to 7.6 mol/kg at 273 K and 100 kPa.	120
pyridinic-N (N-6), pyrrole/pyridine-N (N-5), and quaternary-N (N-Q)	coconut shell	carbonization of coconut shell followed by urea modification and K <sub>2</sub> CO <sub>3</sub> activation at 600 °C (K <sub>2</sub> CO <sub>3</sub> /precursor ratio of 3)	SSA 1082 m <sup>2</sup> g <sup>-1</sup> , nitrogen content (wt%) 2.74	CO <sub>2</sub> capture capacity of 3.71 mmol/g at 25 °C	121
	Cellulose	Reaction with co-pyrolysis experiments of cellulose and nitrogen carriers (urea and chitosan), nitrogen carrier/(cellulose + nitrogen carrier) = 40%-60%, at 350-750 °C.	The N groups on nitrogen-containing biochar were mainly Pyridine nitrogen and pyrrole nitrogen groups, the N atom was fixed in the carbon lattice.	Donor performance and conductivity of carbon materials.	122

237 **ssa** specific surface area

238

239

240

241

### 3.7. Modification of biochar with catalyst nanoparticles

Biochar is a very versatile platform for nanocatalyst immobilization. This is a hot topic of interest for environmental and other applications such as organic synthesis. Our primary goal was to focus on biochar with molecular and macromolecular compounds. However, as most of the nanocatalysts immobilized on biochar were obtained from metal ion compounds, this section closes the review with a logical sequence when one considers the size: molecules, macromolecules, and nano- or macroparticles. Figure 18 summarizes the main methods of preparation of biochar loaded with catalytic particles:

-Method (i) consists in impregnating the initial biomass with catalyst precursor prior to pyrolysis. This process yields biochar powder impregnated with nanoparticles.<sup>37, 123-125</sup>

-Method (ii) concerns the deposition of catalyst precursor onto prefabricated biochar, followed by in situ reductive process to obtain biochar-immobilized nanocatalysts.<sup>8, 88, 126</sup>

-Method (iii) is based on the simple mixture of prefabricated biochar and catalysts.<sup>7, 127</sup>

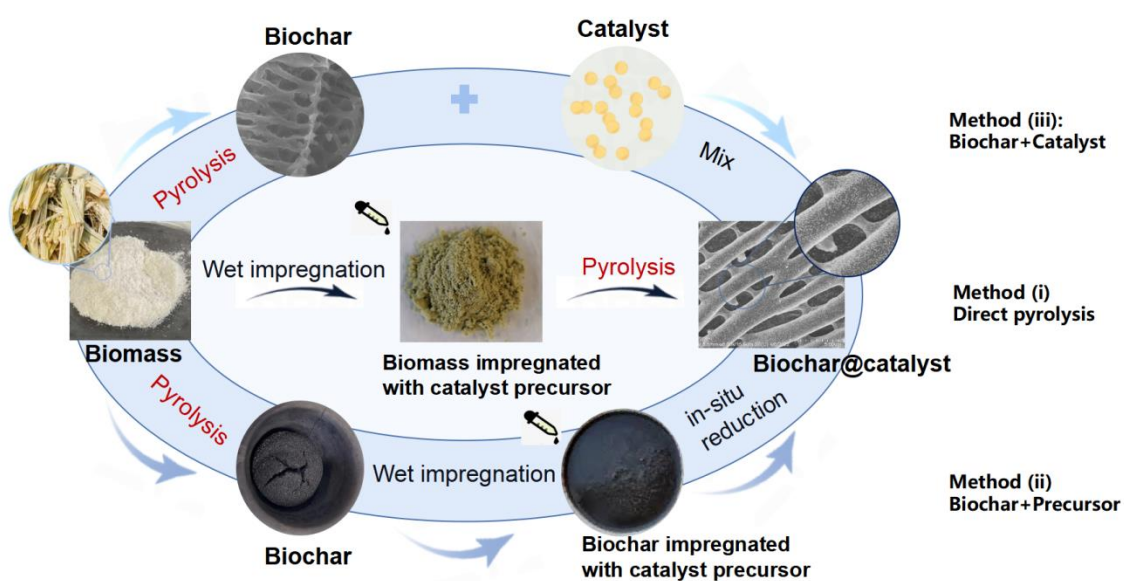


**Figure 18.** Main methods of surface modification of biochar with immobilized nanocatalysts.

From the own experience of the authors, Method (i) yields no loss and evenly dispersed nanoparticles in the nanoscale regime. It requires simple wet impregnation prior to pyrolysis. Method (ii) usually combines two processes: pyrolysis in dry conditions, followed by adsorption of metal ions and their in situ reduction by “beaker chemistry”. Method (iii) is perhaps the one that is amenable to pilot or higher scale process as it requires mixing two preformed components of the final composites. However, agglomerated catalyst nanoparticles might be difficult to disperse, with small size, over the biochar surface. Table 6 provides the summarized experimental work for the

267  
268  
269

preparation of catalyst-modified biochar and potential applications of the shortlisted systems.

270 **Table 6.** Shortlisted biochar@catalyst composites prepared by main three routes, their properties and applications.

Preparation Method	Biomass	Biochar@Catalyst (size of catalyst)	Synthesis procedure	Pollutant removal efficiency	Refs.
<b>Method (i)</b> Pyrolysis of catalyst precursor-impregnated biomass	Olive pit powder (OP)	Biochar@CuNi (10-20 nm agglomerated into raspberry-shaped particles of CuNi)	Pyrolysis of OP pre-modified with citric acid, then impregnated with copper and nickel Ni nitrates before pyrolysis at 400 °C (1h/N <sub>2</sub> ).	Methyl Orange (MO) dye reduction using NaBH <sub>4</sub> . R <sub>eff</sub> = 75% within 90 min.	<sup>128</sup>
	Maize straw (MS)	Biochar@Cu(0) (Cu(0) nanoparticle size: NA)	1g MS was modified with 2.5 mmol CuCl <sub>2</sub> ·2H <sub>2</sub> O prior to pyrolysis at 700 °C (under N <sub>2</sub> . Pyrolysis duration: NA)	Enrofloxacin mineralization using 2 mmol/L PMS. Complete removal: 30 min for 10 mg/L of ENR at pH 3, using 0.3 g/L catalyst.	<sup>125</sup>
	Brewer spent grain (BSG)	Biochar@Ag-Cu (Ag-Cu nanoparticle size ≤ 80 nm)	1g of BSG powder was impregnated with 169.8 mg silver nitrate and 241.6 mg copper (II) nitrate trihydrate in 10 ml aqueous solution. The impregnated BSG powder was dried at 60°C overnight and pyrolyzed at 500 °C (1h/N <sub>2</sub> ).	Study of the dual mineralization of MO and Methylene Blue (MB) dye mixture via advanced oxidation process. Total mineralization was observed for MO in less than 6 hours.	<sup>124</sup>
<b>Method (ii)</b> In situ synthesis of nanocatalyst in the presence of Biochar	Sugarcane bagasse (SCB)	Biochar-SO <sub>3</sub> @AgCu (AgCu < 100 nm)	Pyrolysis of macerated SCB at 500 °C (1h/H <sub>2</sub> 5%/N <sub>2</sub> 95%), followed by arylation with diazonium salt in acidic medium. Biogenic AgCu nanocatalyst was prepared in the presence of the arylated biochar.	Mineralization of Malachite Green (MG) in the presence of H <sub>2</sub> O <sub>2</sub> . R <sub>eff</sub> = 80% within 50 min.	<sup>88</sup>
	<i>Camellia oleifera</i> shell powder	Biochar@Ce-Ag	CSP mixed with KOH then pyrolyzed at 837 °C. 1g biochar was stirred with 0.458 g AgNO <sub>3</sub> , and 0.375 g Ce(NO <sub>3</sub> ) <sub>3</sub> ·6H <sub>2</sub> O for 1h, dried and pyrolyzed at 600 °C.	Sulfathiazole adsorption at 25 °C = 262 mg/g Biochar@Ce-Ag. Adsorption on pure CSP biochar = 42.4 mg/g.	<sup>126</sup>
<b>Method (iii):</b> Preparation of Biochar@Catalyst by mixing Biochar and catalyst	Pomegranate shell	Biochar@CuNi	Biochar was prepared in two steps: hydrothermal treatment at 180 °C/24 h followed by pyrolysis of the resulting hydrochar at 500 °C (1h). CuNi bimetallic catalyst was prepared from equimolar mixture of copper and nickel chlorides. 0.5	Application to the catalysis of A3 coupling reaction (A3: coupling reaction of an aldehyde, an amine, and a terminal alkyne). Optimal conditions were found in toluene, at 80 °C at reflux, for 8h. Benzaldehyde (1.0 mmol), Morpholine (1.2 mmol) and Phenylacetylene	<sup>7</sup>

---

Bamboo	ZnO/Biochar	<p>g CuNi and 1 g biochar were mixed in 30 mL water under sonication for 30 min. The mixture was treated in autoclave at 140 °C for 12 h. The biochar@CuNi was dried at 80 °C for 4h.</p> <p>15 g bamboo was pyrolyzed, 600°C, 2h, N<sub>2</sub>. Biochar and ZnO particles were ball milled.</p>	<p>(1.5 mmol) were reacted in the presence of 20 mg Biochar@CuNi. Highest yield= 88 %.</p> <p>Photo-catalytic degradation of MB (160 mg/g). Removal efficiency= 95.19%</p>
--------	-------------	---	--

---

271

#### 4. Conclusion

In this review, we have summarized the essential findings on the (macro)molecular and nanoparticulate levels of biochar surface treatment. We have covered the modifications of numerous biochar types with silane and titanate coupling agents, aryl diazonium salts, ionic and non-ionic surfactants, nitrogen-containing compounds, and nanocatalysts. Nitrogen species could be a polymerizable monomer (aniline derivatives) or a preformed polymer such as polyethyleneimine (PEI) adsorbed from an alcoholic solution.

One could draw numerous conclusions:

-in general, surface modification reduces the specific surface area and porous volume, but it is worth it because it imparts functionalities that unmodified biochar samples do not possess

-silanization requires rich oxygen functionalities at the surface which could be obtained at moderate pyrolysis temperature, or after oxidization of the biochar.

-titanate could be envisaged to create new biochar-polymer composites, if the primary intention is not to design biochar-titania photocatalysts

-aryl diazonium salts could be regarded as new coupling agents in materials surface chemistry as witnessed over the last three decades; their use to modify biochar particles is recent and very encouraging. Some of us have demonstrated that surface modification is limited by steric hindrance effects of the aryl group, and change in the carbon structure of the biochar is significant at low initial diazonium concentration

-modification with non-ionic and ionic surfactant adsorbed layers influences the textural characteristics of biochar, as well as acid-basic and hydrophilic-hydrophobic properties of its surface, changing the affinity for other substances present in the aqueous phase. The electrostatic, hydrogen bonds,  $\pi$ - $\pi$  electrons, and hydrophobic interactions are responsible for the surfactant molecules binding and can result in the formation of more complex surface structures, such as surfactant-adsorbate multilayers and micelles.



300  
301 -the preparation of biochar-polyaniline composites are investigated by several  
302 researchers, particularly for the fabrication of supercapacitors, whereas poly(2-  
303 aminothiophenol) could be a remarkable alternative to provide surface-immobilized NH  
304 and SH groups able to chelate metal ions, for environmental remediation issues

305 -polyethyleneimine is a nitrogen-rich polymer and could be coated on biochar particles  
306 by adsorption from methanol or ethanol solution. Tight, covalent immobilization and  
307 crosslinking require using organic coupling agents such as glutaraldehyde.

308 -other attractive nitrogen-modification of biochar rest on the doping with ammonium  
309 persulfate or urea prior to pyrolysis, with a result of enhancing pyridinic, pyrrolic, and  
310 graphitic nitrogen in the biochar structure.

311 -finally, there are numerous routes for catalytic nanoparticle modification of biochar,  
312 groups in three major methods. They provide surface-immobilized nanoparticles, but  
313 pyrolysis of catalyst precursor-impregnated biomass seems to provide narrow size  
314 distribution nanoparticles that are immobilized both at the surface and into the large  
315 pores of the biochar.

316 These are the most investigated surface modifiers but others are worth deeper insight,  
317 *e.g.* mercaptoethanol<sup>129</sup> and vitamin-B6.<sup>130</sup> Nevertheless, all in one, there is much to  
318 anticipate from surface chemical modification of biochar in the coming years. Surface  
319 modification imparts remarkable new functionalities such as pollutant adsorption,  
320 immobilization of catalysts, and improved energy storage properties, to name but a few.

321 Concerning bulk, surface, and textural properties, we witnessed recurrent utilization of  
322 XPS, Raman and FTIR, XRD, nitrogen adsorption (for BET and porous volume), and  
323 TGA. Other techniques are also applied in the case of specific applications such as energy  
324 storage, namely DC voltage-current measurements, and cyclic voltammetry. Ironically,  
325 we have noted that the biochar topic tackles the valorization of wastes, with zero value,  
326 but requires a high number of analytical techniques, which is excessively costly for  
327 academic laboratories.

328 From the above, the conversion of agro- and other organic wastes into biochar is a very  
329 hot topic with over 5500 publications per year. This will continue to grow in this era of  
330 economic crisis, on the one hand, and to address some of the 17 sustainable development  
331 goals, on the other hand. We thus expect even more publications on the topic and the  
332 valorization of numerous other wastes. There are already, and there will be new regional  
333 niches from North to South to valorize biomasses such as Douglas fir,<sup>101</sup> brewer spent  
334 grain,<sup>124</sup> sugarcane bagasse,<sup>88</sup> olive<sup>128, 131</sup> and date<sup>132</sup> stones, durian,<sup>102</sup> .... However, more  
335 rationality is needed to select which agrowaste is worth the thermochemical  
336 transformation into biochar, by determining the initial cellulose-hemicellulose-lignin  
337 composition as their thermochemical transformation yields biochars with completely  
338 different properties and thus different potential applications, for example as electrode  
339 materials.<sup>13</sup> Pyrolysis is interesting and offers advantages, but for other applications,  
340 hydrochars could be a solution because the treatment is faster, and the process might  
341 provide extraction of phytochemical useful for reductive reaction processes,<sup>15</sup> and also  
342 carbon dots.<sup>133</sup> Recently, microwave heating has emerged as an alternative for the  
343 fabrication of carbonaceous chars, with low energy cost of preparation, and remarkable  
344 properties.<sup>132</sup> Yet, when it comes to surface modification, this review has indicated  
345 numerous opportunities, but also challenges to overcome, such as the balance between  
346 surface chemistry and textural properties in order to achieve the desired end properties  
347 and performances.

348  
349  
350 **Authors' contributions:** Conceptualization (AMK, MW, MMC); Methodology (MMC, MW);  
351 Validation (all authors); Writing-Original Draft (AMK, MW, MMC); Writing - Review & Editing  
352 (all authors); Resources (MMC, AMK, MW); Supervision (MMC); Funding acquisition (AMK, MT,  
353 MMC, AKB, YS).

#### 354 355 **Funding**

356 AMK and MMC would like to thank the French Government for funding AMK's contribution

through a fellowship granted by the French Embassy in Egypt (Institut Francais d’Egypte). We thank the China Scholarship Council for the provision of PhD scholarship to Mengqi Tang (No 202008310221). AKB thanks WBI for the provision of a grant “Bourse Wallonie-Bruxelles International Excellence World (N° imputation – 101386, and Article Budgetaire – 33.01.00.07)”.

**Institutional Review Board Statement:** Not applicable

**Informed Consent Statement:** Not applicable.

**Data Availability Statement:** Not applicable

**Conflict of interest:** the authors declare no conflict of interest

## References

- 1 S. Adhikari, W. Timms, M. A. P. Mahmud, *Science of The Total Environment* **2022**, *851*, 158043 <https://doi.org/10.1016/j.scitotenv.2022.158043>.
- 2 S. Wijitkosum, *International Soil and Water Conservation Research* **2022**, *10*, 335-341 <https://doi.org/10.1016/j.iswcr.2021.09.006>.
- 3 M. Harussani, S. Sapuan, *Chemistry Africa* **2021**, 1-17.
- 4 H. Liu, Y. Liu, X. Li, X. Zheng, X. Feng, A. Yu, in *Book Adsorption and Fenton-like Degradation of Ciprofloxacin Using Corncob Biochar-Based Magnetic Iron&ndash;Copper Bimetallic Nanomaterial in Aqueous Solutions*, ed., ed. by Editor, City, **2022**, Vol. 12, Chap. Chapter.
- 5 A. Mukherjee, N. Goswami, D. Dhak, *Chemistry Africa* **2022**, 10.1007/s42250-022-00467-5.
- 6 H. Rodríguez Molina, J. L. Santos Muñoz, M. I. Domínguez Leal, T. R. Reina, S. Ivanova, M. Á. Centeno Gallego, J. A. Odriozola, *Frontiers in Chemistry* **2019**, *7*, 10.3389/fchem.2019.00548.
- 7 M. Zarei, K. Saidi, H. Sheibani, *Biomass Conversion and Biorefinery* **2022**, 10.1007/s13399-022-03544-4.
- 8 J. L. Santos, L. M. Sanz-Moral, A. Aho, S. Ivanova, D. Y. Murzin, M. A. Centeno, *Biomass and Bioenergy* **2022**, *163*, 106504 <https://doi.org/10.1016/j.biombioe.2022.106504>.
- 9 M. Bartoli, R. Arrigo, G. Malucelli, A. Tagliaferro, D. Duraccio, *Polymers* **2022**, *14*, 2506.
- 10 N. Bélanger, S. Prasher, M.-J. Dumont, *Polymer-Plastics Technology and Materials* **2023**, *62*, 54-75 [10.1080/25740881.2022.2089584](https://doi.org/10.1080/25740881.2022.2089584).
- 11 M. M. Harussani, S. M. Sapuan, G. Nadeem, T. Rafin, W. Kirubaanand, *Defence Technology* **2022**, *18*, 1281-1300 <https://doi.org/10.1016/j.dt.2022.03.006>.
- 12 T. Huggins, H. Wang, J. Kearns, P. Jenkins, Z. J. Ren, *Bioresource technology* **2014**, *157*, 114-119.
- 13 S. Tabac, D. Eisenberg, *Current Opinion in Electrochemistry* **2021**, *25*, 100638 <https://doi.org/10.1016/j.coelec.2020.09.005>.
- 14 Y. Snoussi, I. Sifaoui, A. M. Khalil, A. K. Bhakta, O. Semyonov, P. S. Postnikov, L. Michely, R. Pires, S. Bastide, J. E.-P. Barroso, J. L. Morales, M. M. Chehimi, *Materials Today Communications* **2022**, *32*, 104126 <https://doi.org/10.1016/j.mtcomm.2022.104126>.
- 15 Y. Snoussi, I. Sifaoui, M. El Garah, A. M. Khalil, J. E. Piñero, M. Jouini, S. Ammar, J. Lorenzo-Morales, M. M. Chehimi, *Waste Management* **2023**, *155*, 179-191 <https://doi.org/10.1016/j.wasman.2022.11.006>.

- 396 16 J. L. Santos, M. A. Centeno, J. A. Odriozola, *Journal of Analytical and Applied Pyrolysis* **2020**, *148*, 104821  
397 <https://doi.org/10.1016/j.jaap.2020.104821>.
- 398 17 H. W. Lee, H. Lee, Y.-M. Kim, R.-s. Park, Y.-K. Park, *Chinese Chemical Letters* **2019**, *30*, 2147-2150  
399 <https://doi.org/10.1016/j.ccllet.2019.05.002>.
- 400 18 U. Kamran, S.-J. Park, *Journal of Cleaner Production* **2021**, *290*, 125776  
401 <https://doi.org/10.1016/j.jclepro.2020.125776>.
- 402 19 R. P. Lopes, D. Astruc, *Coordination Chemistry Reviews* **2021**, *426*, 213585.
- 403 20 D. Luo, L. Wang, H. Nan, Y. Cao, H. Wang, T. V. Kumar, C. Wang, *Environmental Chemistry Letters* **2022**,  
404 10.1007/s10311-022-01519-5.
- 405 21 L. Goswami, A. Kushwaha, S. R. Kafle, B.-S. Kim, *Catalysts* **2022**, *12*, 817.
- 406 22 D. C. C. d. S. Medeiros, C. Nzediegwu, C. Benally, S. A. Messele, J.-H. Kwak, M. A. Naeth, Y. S. Ok, S. X. Chang,  
407 M. Gamal El-Din, *Science of The Total Environment* **2022**, *809*, 151120  
408 <https://doi.org/10.1016/j.scitotenv.2021.151120>.
- 409 23 M. Tripathi, J. N. Sahu, P. Ganesan, *Renewable and Sustainable Energy Reviews* **2016**, *55*, 467-481.
- 410 24 H. Tan, C. T. Lee, P. Y. Ong, K. Y. Wong, C. P. C. Bong, C. Li, Y. Gao, *IOP Conference Series: Materials Science  
411 and Engineering* **2021**, *1051*, 012075 10.1088/1757-899X/1051/1/012075.
- 412 25 J. O. Ighalo, F. U. Iwuchukwu, O. E. Eyankware, K. O. Iwuozor, K. Olotu, O. C. Bright, C. A. Igwegbe, *Clean  
413 Technologies and Environmental Policy* **2022**, *24*, 2349-2363 10.1007/s10098-022-02339-5.
- 414 26 E. Pawelczyk, I. Wysocka, J. Gębicki, in *Book Pyrolysis Combined with the Dry Reforming of Waste Plastics as  
415 a Potential Method for Resource Recovery&mdash;A Review of Process Parameters and Catalysts*, ed., ed. by Editor,  
416 City, **2022**, Vol. 12, Chap. Chapter.
- 417 27 S. Yu, X. Yang, P. Zhao, Q. Li, H. Zhou, Y. Zhang, *Journal of the Energy Institute* **2022**, *101*, 194-200  
418 <https://doi.org/10.1016/j.joei.2022.01.013>.
- 419 28 M. Selvam S, B. Paramasivan, *Chemosphere* **2022**, *286*, 131631  
420 <https://doi.org/10.1016/j.chemosphere.2021.131631>.
- 421 29 S.-Y. Jeong, C.-W. Lee, J.-U. Lee, Y.-W. Ma, B.-S. Shin, in *Book Laser-Induced Biochar Formation through 355  
422 nm Pulsed Laser Irradiation of Wood, and Application to Eco-Friendly pH Sensors*, ed., ed. by Editor, City, **2020**, Vol.  
423 10, Chap. Chapter.
- 424 30 S. You, Y. S. Ok, S. S. Chen, D. C. W. Tsang, E. E. Kwon, J. Lee, C.-H. Wang, *Bioresource Technology* **2017**, *246*,  
425 242-253 <https://doi.org/10.1016/j.biortech.2017.06.177>.
- 426 31 L. Li, M. Yang, Q. Lu, W. Zhu, H. Ma, L. Dai, *Bioresource Technology* **2019**, *294*, 122142  
427 <https://doi.org/10.1016/j.biortech.2019.122142>.
- 428 32 A. Kumar, K. Saini, T. Bhaskar, *Bioresource Technology* **2020**, *310*, 123442  
429 <https://doi.org/10.1016/j.biortech.2020.123442>.
- 430 33 A. Pandey, T. Bhaskar, M. Stöcker, R. Sukumaran, **2015**.
- 431 34 T. Dutta, E. Kwon, S. S. Bhattacharya, B. H. Jeon, A. Deep, M. Uchimiya, K.-H. Kim, *GCB Bioenergy* **2017**, *9*,  
432 990-1004 <https://doi.org/10.1111/gcbb.12363>.
- 433 35 C. Wang, Y. Wang, H. M. S. K. Herath, *Organic Geochemistry* **2017**, *114*, 1-11  
434 <https://doi.org/10.1016/j.orggeochem.2017.09.001>.
- 435 36 A. K. Bhakta, Y. Snoussi, M. E. Garah, S. Ammar, M. M. Chehimi, in *Book Brewer&rsquo;s Spent Grain Biochar:  
436 Grinding Method Matters*, ed., ed. by Editor, City, **2022**, Vol. 8, Chap. Chapter.
- 437 37 M. Tang, Y. Snoussi, A. Bhakta, M. El Garah, A. Khalil, S. Ammar, M. Chehimi, **2022**.

- 438 38 D. Li, L. Zhao, X. Cao, Z. Xiao, H. Nan, H. Qiu, *Chemical Engineering Journal* **2021**, *406*, 126856  
439 <https://doi.org/10.1016/j.cej.2020.126856>.
- 440 39 X. Pan, Z. Gu, W. Chen, Q. Li, *Science of The Total Environment* **2021**, *754*, 142104.
- 441 40 M. M. Chehimi, J. Pinson, F. Mousli, *Aryl Diazonium Salts and Related Compounds: Surface Chemistry and*  
442 *Applications*. Editor, Springer Nature, **2022**.
- 443 41 C. Li, Y. Gao, A. Li, L. Zhang, G. Ji, K. Zhu, X. Wang, Y. Zhang, *Environmental Pollution* **2019**, *254*, 113005  
444 <https://doi.org/10.1016/j.envpol.2019.113005>.
- 445 42 F. Asgharzadeh, R. R. Kalantary, M. Gholami, A. J. Jafari, M. Kermani, H. Asgharnia, *Biomass Conversion and*  
446 *Biorefinery* **2021**, 10.1007/s13399-021-01685-6.
- 447 43 X. Wang, J. Feng, Y. Cai, M. Fang, M. Kong, A. Alsaedi, T. Hayat, X. Tan, *Science of The Total Environment*  
448 **2020**, *708*, 134575 <https://doi.org/10.1016/j.scitotenv.2019.134575>.
- 449 44 S. Detriche, A. K. Bhakta, P. N'Twali, J. Delhalle, Z. Mekhalif, in *Book Assessment of Catalyst Selectivity in*  
450 *Carbon-Nanotube Silylation*, ed., ed. by Editor, City, **2020**, Vol. 10, Chap. Chapter.
- 451 45 P. Walker, *Handbook of adhesive technology* **2003**, *2*, 205-221.
- 452 46 Y. Lan, W. Wang, *Advances in Polymer Technology* **2018**, *37*, 1979-1986 <https://doi.org/10.1002/adv.21856>.
- 453 47 M. Zhang, H. Zhu, B. Xi, Y. Tian, X. Sun, H. Zhang, B. Wu, in *Book Surface Hydrophobic Modification of Biochar*  
454 *by Silane Coupling Agent KH-570*, ed., ed. by Editor, City, **2022**, Vol. 10, Chap. Chapter.
- 455 48 H. Bamdad, K. Hawboldt, S. MacQuarrie, *Energy & Fuels* **2018**, *32*, 11742-11748  
456 10.1021/acs.energyfuels.8b03056.
- 457 49 P. Moradi, M. Hajjami, *RSC Advances* **2022**, *12*, 13523-13534 10.1039/D1RA09350A.
- 458 50 P. Moradi, M. Hajjami, *New Journal of Chemistry* **2021**, *45*, 2981-2994 10.1039/D0NJ04990E.
- 459 51 Y. Huang, S. Xia, J. Lyu, J. Tang, *Chemical Engineering Journal* **2019**, *360*, 1646-1655  
460 <https://doi.org/10.1016/j.cej.2018.10.231>.
- 461 52 W. Ran, H. Zhu, X. Shen, Y. Zhang, *Construction and Building Materials* **2022**, *329*, 127057  
462 <https://doi.org/10.1016/j.conbuildmat.2022.127057>.
- 463 53 G. Devi, N. Nagabhooshanam, M. Chokkalingam, S. K. Sahu, *Polymer Composites* **2022**, *43*, 5996-6003  
464 <https://doi.org/10.1002/pc.26898>.
- 465 54 B. Wu, B. Xi, X. He, X. Sun, Q. Li, Q. Ouche, H. Zhang, C. Xue, in *Book Methane Emission Reduction Enhanced*  
466 *by Hydrophobic Biochar-Modified Soil Cover*, ed., ed. by Editor, City, **2020**, Vol. 8, Chap. Chapter.
- 467 55 Y. Qin, B. Xi, X. Sun, H. Zhang, C. Xue, B. Wu, *Frontiers in Bioengineering and Biotechnology* **2022**, *10*,  
468 10.3389/fbioe.2022.905466.
- 469 56 K. Sheng, S. Zhang, S. Qian, C. A. Fontanillo Lopez, *Composites Part B: Engineering* **2019**, *165*, 174-182  
470 <https://doi.org/10.1016/j.compositesb.2018.11.139>.
- 471 57 P. Moradi, M. Hajjami, F. Valizadeh-Kakhki, *Applied Organometallic Chemistry* **2019**, *33*, e5205  
472 <https://doi.org/10.1002/aoc.5205>.
- 473 58 H. Li, L. Sun, W. Li, *Journal of Materials Science* **2022**, *57*, 13845-13870 10.1007/s10853-022-07488-y.
- 474 59 Y. Lu, X. Li, C. Wu, S. Xu, *Journal of Alloys and Compounds* **2018**, *750*, 197-205  
475 <https://doi.org/10.1016/j.jallcom.2018.03.301>.
- 476 60 N. W. Elshereksi, M. Ghazali, A. Muchtar, C. H. Azhari, *Dental materials journal* **2017**, 2016-014.
- 477 61 B. Ali Sabri, S. Meenaloshini, N. M. Abreeza, A. N. Abed, *Materials Today: Proceedings* **2021**,  
478 <https://doi.org/10.1016/j.matpr.2021.06.340>.
- 479 62 Y. Zeng, Y. Xue, L. Long, J. Yan, *Water, Air, & Soil Pollution* **2019**, *230*, 50 10.1007/s11270-019-4104-2.

- 480 63 K. D. Cai, W. F. Mu, in *Book Activated carbon modified by titanate coupling agent for supercapacitor*, ed., ed.  
481 by Editor, Trans Tech Publ, City, **2012**, Vol. 347, Chap. Chapter, pp. 3649-3652.
- 482 64 X. Li, C. Gan, Z. Han, H. Yan, D. Chen, W. Li, H. Li, X. Fan, D. Li, M. Zhu, *Carbon* **2020**, *165*, 238-250  
483 <https://doi.org/10.1016/j.carbon.2020.04.038>.
- 484 65 M. Shahverdi, E. Kouhgard, B. Ramavandi, *Data in Brief* **2016**, *9*, 163-168  
485 <https://doi.org/10.1016/j.dib.2016.08.051>.
- 486 66 L. Mathurasa, S. Damrongsiri, *Applied Environmental Research* **2017**, *39*, 11-22.
- 487 67 M. Wiśniewska, P. Nowicki, T. Urban, *Journal of Molecular Liquids* **2021**, *332*, 115872  
488 <https://doi.org/10.1016/j.molliq.2021.115872>.
- 489 68 F. Wang, Q. Zeng, W. Su, M. Zhang, L. Hou, Z.-L. Wang, *Journal of Chemistry* **2019**, *2019*, 2428505  
490 [10.1155/2019/2428505](https://doi.org/10.1155/2019/2428505).
- 491 69 C. Kosaiyakanon, S. Kungsanant, *Environment and Natural Resources Journal* **2019**, *18*, 21-32.
- 492 70 X. Mi, G. Li, W. Zhu, L. Liu, *Journal of Chemistry* **2016**, *2016*.
- 493 71 M. Wiśniewska, P. Nowicki, *Colloids and Surfaces A: Physicochemical and Engineering Aspects* **2020**, *585*,  
494 [124179](https://doi.org/10.1016/j.colsurfa.2019.124179) <https://doi.org/10.1016/j.colsurfa.2019.124179>.
- 495 72 A. K. Anas, S. Y. Pratama, A. Izzah, M. A. Kurniawan, *2021* **2021**, *8* 10.9767/bcrec.16.1.10323.188-195.
- 496 73 A. K. Anas, A. Izzah, S. Y. Pratama, F. I. Fajarwati, *AIP Conference Proceedings* **2020**, *2229*, 030024  
497 [10.1063/5.0002675](https://doi.org/10.1063/5.0002675).
- 498 74 W. Que, L. Jiang, C. Wang, Y. Liu, Z. Zeng, X. Wang, Q. Ning, S. Liu, P. Zhang, S. Liu, *Journal of Environmental*  
499 *Sciences* **2018**, *70*, 166-174 <https://doi.org/10.1016/j.jes.2017.11.027>.
- 500 75 H. He, W. Li, H. Deng, L. Kang, R. Qiu, X. Li, W. Liu, Z. Meng, *Desalination and Water Treatment* **2019**, *148*,  
501 195-201.
- 502 76 M. Wiśniewska, P. Nowicki, K. Szewczuk-Karpisz, M. Gęca, K. Jędruchiewicz, P. Oleszczuk, *Separation and*  
503 *Purification Technology* **2021**, *276*, 119297 <https://doi.org/10.1016/j.seppur.2021.119297>.
- 504 77 Z. Hua, S. Wan, L. Sun, Z. Yu, X. Bai, *Journal of Chemical Technology & Biotechnology* **2018**, *93*, 3044-3055  
505 <https://doi.org/10.1002/jctb.5663>.
- 506 78 P. Griess, *Annalen* **1858**, *106*, 123-125.
- 507 79 S. V. Heines, *Journal of Chemical Education* **1958**, *35*, 187 [10.1021/ed035p187](https://doi.org/10.1021/ed035p187).
- 508 80 F. Mo, G. Dong, Y. Zhang, J. Wang, *Organic & Biomolecular Chemistry* **2013**, *11*, 1582-1593  
509 [10.1039/C3OB27366K](https://doi.org/10.1039/C3OB27366K).
- 510 81 A. A. Mohamed, Z. Salmi, S. A. Dahoumane, A. Mekki, B. Carbonnier, M. M. Chehimi, *Advances in colloid and*  
511 *interface science* **2015**, *225*, 16-36.
- 512 82 P. Mirzaei, S. Bastide, A. Aghajani, J. Bourgon, E. Leroy, J. Zhang, Y. Snoussi, A. Bensghaier, O. Hamouma, M.  
513 M. Chehimi, *Langmuir* **2019**, *35*, 14428-14436.
- 514 83 A. S. A. Ali H. Jawad, Lee D. Wilson, Syed Shatir A. Syed-Hassan, Zeid A. AlOthman, Mohammad Rizwan Khan,  
515 *Chinese Journal of Chemical Engineering* **2021**, *32*, 281-290 [10.1016/j.cjche.2020.09.070](https://doi.org/10.1016/j.cjche.2020.09.070).
- 516 84 M. H. Abdel-Aziz, E. Z. El-Ashtoukhy, M. Bassyouni, A. F. Al-Hossainy, E. M. Fawzy, S. M. S. Abdel-Hamid, M. S.  
517 Zoromba, *Carbon Letters* **2021**, *31*, 863-878 [10.1007/s42823-020-00187-1](https://doi.org/10.1007/s42823-020-00187-1).
- 518 85 A. M. Khalil, R. Msaadi, W. Sassi, I. Ghanmi, R. Pires, L. Michely, Y. Snoussi, A. Chevillot-Biraud, S. Lau-Truong,  
519 M. M. Chehimi, *Carbon Letters* **2022**, *32*, 1519-1529 [10.1007/s42823-022-00374-2](https://doi.org/10.1007/s42823-022-00374-2).
- 520 86 A. L. Rodd, M. A. Creighton, C. A. Vaslet, J. R. Rangel-Mendez, R. H. Hurt, A. B. Kane, *Environmental Science &*  
521 *Technology* **2014**, *48*, 6419-6427 [10.1021/es500892m](https://doi.org/10.1021/es500892m).

- 522 87 A. Bensghaïer, Z. Salmi, B. Le Droumaguet, A. Mekki, A. A. Mohamed, M. Beji, M. M. Chehimi, *Surface and*  
523 *Interface Analysis* **2016**, *48*, 509-513.
- 524 88 Y. Snoussi, M. El Garah, A. M. Khalil, S. Ammar, M. M. Chehimi, *Applied Organometallic Chemistry* **2022**, *36*,  
525 e6885 <https://doi.org/10.1002/aoc.6885>.
- 526 89 K. Malins, V. Kampars, J. Brinks, I. Neibolte, R. Murnieks, *Applied Catalysis B: Environmental* **2015**, *176-177*,  
527 553-558 <https://doi.org/10.1016/j.apcatb.2015.04.043>.
- 528 90 S. Niu, Y. Ning, C. Lu, K. Han, H. Yu, Y. Zhou, *Energy Conversion and Management* **2018**, *163*, 59-65  
529 <https://doi.org/10.1016/j.enconman.2018.02.055>.
- 530 91 T. Zhang, H. Wei, J. Gao, S. Chen, Y. Jin, C. Deng, S. Wu, H. Xiao, W. Li, *Molecular Catalysis* **2022**, *517*, 112034  
531 <https://doi.org/10.1016/j.mcat.2021.112034>.
- 532 92 A. Malaika, K. Ptaszyńska, M. Kozłowski, *Fuel* **2021**, *288*, 119609 <https://doi.org/10.1016/j.fuel.2020.119609>.
- 533 93 L. J. Konwar, P. Mäki-Arvela, J.-P. Mikkola, *Chemical Reviews* **2019**, *119*, 11576-11630  
534 [10.1021/acs.chemrev.9b00199](https://doi.org/10.1021/acs.chemrev.9b00199).
- 535 94 Y. Zhong, Q. Deng, P. Zhang, J. Wang, R. Wang, Z. Zeng, S. Deng, *Fuel* **2019**, *240*, 270-277  
536 <https://doi.org/10.1016/j.fuel.2018.11.152>.
- 537 95 Z. Wan, Y. Sun, D. C. W. Tsang, E. Khan, A. C. K. Yip, Y. H. Ng, J. Rinklebe, Y. S. Ok, *Chemical Engineering*  
538 *Journal* **2020**, *401*, 126136 <https://doi.org/10.1016/j.cej.2020.126136>.
- 539 96 N. Kasera, P. Kolar, S. G. Hall, *Biochar* **2022**, *4*, 17 [10.1007/s42773-022-00145-2](https://doi.org/10.1007/s42773-022-00145-2).
- 540 97 Z. Lin, R. Wang, S. Tan, K. Zhang, Q. Yin, Z. Zhao, P. Gao, *Journal of Environmental Management* **2023**, *334*,  
541 117503 <https://doi.org/10.1016/j.jenvman.2023.117503>.
- 542 98 R. Chatterjee, B. Sajjadi, W.-Y. Chen, D. L. Mattern, N. O. Egiebor, N. Hammer, V. Raman, *Energy & Fuels*  
543 **2019**, *33*, 2366-2380 [10.1021/acs.energyfuels.8b03583](https://doi.org/10.1021/acs.energyfuels.8b03583).
- 544 99 M. Shahabi Nejad, H. Sheibani, *Journal of Environmental Chemical Engineering* **2022**, *10*, 107363  
545 <https://doi.org/10.1016/j.jece.2022.107363>.
- 546 100 R. C. Thomas, J. E. Houston, R. M. Crooks, T. Kim, T. A. Michalske, *Journal of the American Chemical Society*  
547 **1995**, *117*, 3830-3834 [10.1021/ja00118a019](https://doi.org/10.1021/ja00118a019).
- 548 101 A. Herath, C. Reid, F. Perez, C. U. Pittman, T. E. Mlsna, *Journal of Environmental Management* **2021**, *296*,  
549 113186 <https://doi.org/10.1016/j.jenvman.2021.113186>.
- 550 102 K. R. Thines, E. C. Abdullah, M. Ruthiraan, N. M. Mubarak, M. Tripathi, *Journal of Analytical and Applied*  
551 *Pyrolysis* **2016**, *121*, 240-257 <https://doi.org/10.1016/j.jaap.2016.08.004>.
- 552 103 D. Thomas, N. B. Fernandez, M. D. Mullassery, R. Surya, *Inorganic Chemistry Communications* **2020**, *119*,  
553 108097 <https://doi.org/10.1016/j.inoche.2020.108097>.
- 554 104 Y. Ma, T. Zhang, P. Zhu, H. Cai, Y. Jin, K. Gao, J. Li, *Science of The Total Environment* **2022**, *821*, 153453  
555 <https://doi.org/10.1016/j.scitotenv.2022.153453>.
- 556 105 Y. Ma, W.-J. Liu, N. Zhang, Y.-S. Li, H. Jiang, G.-P. Sheng, *Bioresource Technology* **2014**, *169*, 403-408  
557 <https://doi.org/10.1016/j.biortech.2014.07.014>.
- 558 106 J. Qu, X. Zhang, F. Bi, S. Wang, X. Zhang, Y. Tao, Y. Wang, Z. Jiang, Y. Zhang, *Environmental Pollution* **2022**,  
559 *313*, 120103 <https://doi.org/10.1016/j.envpol.2022.120103>.
- 560 107 M. Gęca, M. Wiśniewska, P. Nowicki, in *Book Simultaneous Removal of Polymers with Different Ionic*  
561 *Character from Their Mixed Solutions Using Herb-Based Biochars and Activated Carbons*, ed., ed. by Editor, City,  
562 **2022**, Vol. 27, Chap. Chapter.

- 563 108 E. Parameswari, R. Kalaiarasi, V. Davamani, T. Ilakiya, P. Kalaiselvi, S. P. Sebastian, in *Biochar and its*  
564 *Application in Bioremediation*, ed. by R. Thapar Kapoor, H. Treichel, M. P. Shah, Springer Nature Singapore,  
565 Singapore, **2021**, pp. 27-48.
- 566 109 H. Tian, C. Huang, P. Wang, J. Wei, X. Li, R. Zhang, D. Ling, C. Feng, H. Liu, M. Wang, Z. Liu, *Bioresource*  
567 *Technology* **2023**, *369*, 128452 <https://doi.org/10.1016/j.biortech.2022.128452>.
- 568 110 Q. Jiang, W. Xie, S. Han, Y. Wang, Y. Zhang, *Colloids and Surfaces A: Physicochemical and Engineering Aspects*  
569 **2019**, *583*, 123962 <https://doi.org/10.1016/j.colsurfa.2019.123962>.
- 570 111 Z. Xiao, Y. Xie, H. Militz, C. Mai, **2010**, *64*, 483-488 doi:10.1515/hf.2010.087.
- 571 112 D. Pandey, A. Daverey, K. Dutta, K. Arunachalam, *Environmental Monitoring and Assessment* **2022**, *194*, 880  
572 10.1007/s10661-022-10563-1.
- 573 113 W. Mao, Y. Zhang, J. Luo, L. Chen, Y. Guan, *Chemosphere* **2022**, *303*, 135254  
574 <https://doi.org/10.1016/j.chemosphere.2022.135254>.
- 575 114 G. S. dos Reis, D. Bergna, A. Grimm, E. C. Lima, T. Hu, M. Naushad, U. Lassi, *Colloids and Surfaces A:*  
576 *Physicochemical and Engineering Aspects* **2023**, *669*, 131493 <https://doi.org/10.1016/j.colsurfa.2023.131493>.
- 577 115 W. Wang, M. Chen, *Journal of Colloid and Interface Science* **2022**, *613*, 57-70  
578 <https://doi.org/10.1016/j.jcis.2022.01.006>.
- 579 116 B. Yu, Y. Man, P. Wang, C. Wu, J. Xie, W. Wang, H. Jiang, L. Zhang, Y. Zhang, L. Mao, L. Zhu, Y. Zheng, X. Liu,  
580 *Ecotoxicology and Environmental Safety* **2023**, *257*, 114908 <https://doi.org/10.1016/j.ecoenv.2023.114908>.
- 581 117 T. Cheng, Y. Bian, J. Li, X. Ma, L. Yang, L. Zhou, H. Wu, *Fuel* **2023**, *334*, 126452  
582 <https://doi.org/10.1016/j.fuel.2022.126452>.
- 583 118 G. Gao, X. Hu, Q. Wang, C. Li, Q. Chen, L. Zhang, W. Gao, K. Ding, Y. Huang, S. Zhang, *Journal of*  
584 *Environmental Chemical Engineering* **2023**, *11*, 109781 <https://doi.org/10.1016/j.jece.2023.109781>.
- 585 119 Y. Zhang, J. Deng, Y. Liu, H. Li, M. Tan, X. Qin, Z. Wu, Z. Huang, X. Li, Q. Lu, *Environmental Science: Water*  
586 *Research & Technology* **2023**, 10.1039/D2EW00985D.
- 587 120 Y. Geng, Y. Du, T. Guo, Y. Zhang, A. H. Bedane, P. Ren, *Case Studies in Thermal Engineering* **2023**, *44*, 102814  
588 <https://doi.org/10.1016/j.csite.2023.102814>.
- 589 121 L. Yue, Q. Xia, L. Wang, L. Wang, H. DaCosta, J. Yang, X. Hu, *Journal of Colloid and Interface Science* **2018**, *511*,  
590 259-267 <https://doi.org/10.1016/j.jcis.2017.09.040>.
- 591 122 W. Zhao, S. Liu, M. Yin, Z. He, D. Bi, *Journal of Analytical and Applied Pyrolysis* **2023**, *169*, 105795  
592 <https://doi.org/10.1016/j.jaap.2022.105795>.
- 593 123 A. M. Khalil, L. Michely, R. Pires, S. Bastide, K. Jlassi, S. Ammar, M. Jaziri, M. Chehimi, *Applied Sciences* **2021**,  
594 *11*, 10.3390/app11188513.
- 595 124 L. Boubkr, A. K. Bhakta, Y. Snoussi, C. Moreira Da Silva, L. Michely, M. Jouini, S. Ammar, M. M. Chehimi, in  
596 *Book Highly Active Ag-Cu Nanocrystal Catalyst-Coated Brewer's Spent Grain Biochar for the Mineralization of*  
597 *Methyl Orange and Methylene Blue Dye Mixture*, ed., ed. by Editor, City, **2022**, Vol. 12, Chap. Chapter.
- 598 125 J. Zhao, T. Chen, C. Hou, B. Huang, J. Du, N. Liu, X. Zhou, Y. Zhang, in *Book Efficient Activation of*  
599 *Peroxydisulfate by Biochar-Loaded Zero-Valent Copper for Enrofloxacin Degradation: Singlet Oxygen-Dominated*  
600 *Oxidation Process*, ed., ed. by Editor, City, **2022**, Vol. 12, Chap. Chapter.
- 601 126 S. He, L. Wu, Y. Zeng, B. Jia, L. Liang, *Materials Today Communications* **2022**, *33*, 104577  
602 <https://doi.org/10.1016/j.mtcomm.2022.104577>.
- 603 127 F. Yu, F. Tian, H. Zou, Z. Ye, C. Peng, J. Huang, Y. Zheng, Y. Zhang, Y. Yang, X. Wei, B. Gao, *Journal of*  
604 *Hazardous Materials* **2021**, *415*, 125511 <https://doi.org/10.1016/j.jhazmat.2021.125511>.



- 605 128 J. Omiri, Y. Snoussi, A. K. Bhakta, S. Truong, S. Ammar, A. M. Khalil, M. Jouini, M. M. Chehimi, *Colloids and*  
606 *Interfaces* **2022**, *6*, 10.3390/colloids6020018.
- 607 129 J. Fan, C. Cai, H. Chi, B. J. Reid, F. Coulon, Y. Zhang, Y. Hou, *Journal of Hazardous Materials* **2020**, *388*, 122037  
608 <https://doi.org/10.1016/j.jhazmat.2020.122037>.
- 609 130 F. Saremi, M. R. Miroliaei, M. Shahabi Nejad, H. Sheibani, *Journal of Molecular Liquids* **2020**, *318*, 114126  
610 <https://doi.org/10.1016/j.molliq.2020.114126>.
- 611 131 N. Ayedi, B. Rzig, N. Bellakhal, *Chemistry Africa* **2023**, 10.1007/s42250-023-00628-0.
- 612 132 H. A. Alharbi, B. H. Hameed, K. D. Alotaibi, S. S. Al-Oud, A. S. Al-Modaihsh, *Frontiers in Environmental Science*  
613 **2022**, *10*, 996953.
- 614 133 K. Jlassi, S. Mallick, A. Eribi, M. M. Chehimi, Z. Ahmad, F. Touati, I. Krupa, *Sensors and Actuators B: Chemical*  
615 **2021**, *328*, 129058.

616

617

618